



UNIVERSITÀ DEGLI STUDI DI PADOVA

Scuola di Ingegneria
Dipartimento di Ingegneria dell'Informazione
Dipartimento di Ingegneria Industriale

Corso di Laurea Magistrale in Bioingegneria

Titolo della tesi

***Structural analysis of the interaction
between different types of stent and
the trachea tissue***

Supervisore: Malvé Mauro

Laureando: Nicola Pinton

Relatore: Pavan Piero

Data: A.A. 2021/2022

Firma laureando

Firma Relatore

Table of contents

| | |
|--|----|
| Abstract | 6 |
| Sommario | 8 |
| CHAPTER 1 | 10 |
| Introduction | 10 |
| 1.1 Tracheal stenosis | 11 |
| 1.2 Stent | 13 |
| 1.2.1 Application | 14 |
| 1.2.2 Sites of application | 15 |
| 1.2.3 Typologies | 17 |
| 1.3 Respiratory System - General | 20 |
| 1.3.1 Anatomy of the respiratory system | 21 |
| 1.3.2 Pulmonary ventilation | 22 |
| 1.3.3 Inspiration | 23 |
| 1.3.4 Exhalation | 23 |
| CHAPTER 2 | 26 |
| Methods | 26 |
| 2.1 Workflow | 27 |
| 2.2 SolidWorks | 27 |
| 2.3 ANSYS | 28 |
| 2.4 ANSYS Workbench | 29 |
| 2.5 MATLAB | 32 |
| Materials | 33 |
| 2.5 Materials | 33 |
| 2.5.1 Tracheal tissue | 34 |
| 2.5.2 Stent Material | 36 |
| 2.6 Geometry | 38 |

| | |
|--|----|
| 2.6.1 Geometry of the trachea | 38 |
| 2.6.2 Geometry of the stent | 40 |
| 2.6.3 Assembly | 44 |
| 2.7 Meshing | 45 |
| 2.7 Boundary Conditions | 47 |
| 2.7.1 Fixed Support | 47 |
| 2.7.2 Elastic Support | 48 |
| 2.7.3 Contact | 48 |
| 2.8 Load | 50 |
| CHAPTER 3 | 52 |
| Results | 52 |
| 3.1 Deformation stent results | 53 |
| 3.2 Stent stress states | 57 |
| 3.3 Alternative materials | 60 |
| 3.4 Circumferential deformation | 61 |
| CHAPTER 4 | 64 |
| Discussion and Conclusion | 64 |
| Bibliography | 66 |

Abstract

This project aims to analyse the deformations and stresses produced in the tracheal tissue when a stent is inserted, to determine the damage produced. Stents are springs as devices. Their placement aims to open the inside of the narrowed trachea to facilitate the passage of air through the trachea. In particular, the stent models analysed in this project are silicon stent models currently being tested at the University of Zaragoza. These models are also compared with a commercial stent made by Novatech, the Dumon. Similarly, to solve biocompatibility problems and for a more similar elastic rigidity with biological tissues, other materials were tested, such as Polyvinyl alcohol (PVA) and Polydimethylsiloxane (PDMS). In this study, we compare three stent models that are similar to each other but with certain modifications in the geometry of the external surface of the product. In fact, the outside of the stents was designed with an upward reinforcing structure that is similar to the typical X-pattern metallic stents. Attention was focused on the stents' structural behaviour, evaluated through a Finite Element Method software. In all the calculations performed during the project, a simplified morphology of a rabbit trachea was simulated, i.e. a section of the trachea was simulated as a cylinder in which two materials, cartilage and muscle, were differentiated. An already present model to simulate the respiratory cycle of a rabbit was drawn from the existing literature. In conclusion, the computational model is capable of designing, analysing and characterizing the device with the constraints and the requirements of the project.

Sommario

Questo progetto mira ad analizzare le deformazioni e le sollecitazioni prodotte nel tessuto tracheale quando viene inserito uno stent, per determinare il danno prodotto. Gli stent sono dispositivi a molla. Il loro inserimento mira ad aprire l'interno della trachea ristretta per facilitare il passaggio dell'aria attraverso la trachea. In particolare, i modelli di stent analizzati in questo progetto sono modelli in silicone attualmente in fase di sperimentazione presso l'Università di Saragozza. Questi modelli vengono confrontati con uno stent commerciale prodotto da Novatech, il Dumon. Allo stesso modo, per risolvere i problemi di biocompatibilità e per ottenere una rigidità elastica più simile a quella dei tessuti biologici, sono stati testati altri materiali, come il Polyvinyl alcohol (PVA) e il Polydimethylsiloxane (PDMS). In questo studio, confrontiamo tre modelli di stent simili tra loro ma con alcune modifiche nella geometria della superficie esterna del prodotto. Infatti, la parte esterna degli stent è stata progettata con una struttura esterna di rinforzo, simile a quella dei tipici stent metallici a X. L'attenzione si è concentrata sul comportamento strutturale degli stent, valutato attraverso un software con metodo agli elementi finiti. In tutti i calcoli eseguiti durante il progetto, è stata simulata una morfologia semplificata della trachea di coniglio, cioè una sezione della trachea è stata simulata come un cilindro in cui sono stati differenziati due materiali, cartilagine e muscolo. Dalla letteratura esistente è stato tratto un modello già presente per simulare il ciclo respiratorio del coniglio.

In conclusione, il modello computazionale è in grado di progettare, analizzare e caratterizzare il dispositivo con i vincoli e i requisiti del progetto.

CHAPTER 1

Introduction

Biomechanics is a scientific discipline that studies the activity of our body, under different circumstances and conditions, and analyses the mechanical consequences that result from our activity, be it in daily life, work, sport, etc. To study the effects of such activity, biomechanics utilises knowledge from mechanics, engineering, anatomy, physiology and other disciplines. Biomechanics is interested in the movement of the human body, mechanical loads and the energies produced by this movement.

The industrial projection of Biomechanics has reached various sectors, serving as the basis for the design and adaptation of numerous products: diagnostic techniques, surgical implants and instruments, prostheses, technical aids for people with disabilities, systems for assessing our activities, instruments and safety systems in the automotive industry, among many others. According to data from the World Health Organisation (WHO), mortality from cancer of the trachea, bronchus and lungs worldwide is among the top 10 causes, ranking third in high-income countries [1]. In many treatments for diseases of the respiratory system, the number of people suffering from respiratory diseases is increasing. Many treatments for diseases of the respiratory system require intubation of the patient. Prolonged intubation increases the risk of tracheal stenosis, which presents as scarring of the tissues of the walls of the trachea. Tracheal stenosis is the most serious complication of respiratory resuscitation with endotracheal ventilation via tracheostomy or nasotracheal intubation [2].

The problems that currently exist for patients with stenosis or obstructive airway disease, for whom the appropriate solution is the implantation of a stent, are well known. In many cases the stent itself, at first a remedy, becomes part of the problem, preventing the proper circulation of air through the trachea.

The purpose of this study is:

- Develop 3D FEM models of three stents and simulate their placement inside the trachea of a rabbit to analyse its biomechanical response in breathing.
- Compare the different geometries of the stents, based on deformation and stress states induced on the tracheal wall.

1.1 Tracheal stenosis

Tracheal stenosis is a condition that can cause death if not treated correctly in time. Patients usually suffer from respiratory distress, such as dyspnoea or even asphyxia [3] [4]. The cause can be idiopathic, congenital, or acquired, with a distinction between benign and malignant. Acquired stenosis occurs due to prolonged endotracheal intubation causing injury to the glottis and subglottis.

These lesions can be caused by the following factors [5] [6]:

1. Inadequate air pressure from the pneumatic balloon of mechanical ventilators. Above the capillary perfusion pressure of the tracheal mucosa, ischaemia, ulceration and chondritis of the tracheal cartilages occur.
2. Incorrect choice of tube diameter used.
3. Duration of intubation.
4. The patient's movement, which increases pressure on the tissue and causes irritation of the mucosa, can lead to stenosis.

In some cases, it can occur due to a foreign body stuck in the trachea, infection, inflammation, or chemical irritation. Even in patients with chronic inflammatory

diseases such as sarcoidosis, Wegener's granulomatosis, polychondritis, etc., benign, or cancerous tumours pressing on the trachea can lead to tracheal stenosis. The increase in the number of acquired tracheal stenoses may be associated with improved patient survival due to modern successful intensive therapies. In fact, most of these are due to stenosis after long-term tracheal intubation and tracheostomy surgery [7] [8].

The management of this obstructive tracheal lesion is a complex problem that requires a targeted approach. Indeed, it requires radical surgical resection. As is well known, this is not always feasible [8] [9]. The number of complicated tracheal lesions, in which resection and anastomosis are unsuccessful or not applicable, increases and the situation requires a solution by endoprosthesis [2] [10] [11]. Whereas tracheal stenosis due to cancer of the oesophagus, which is considered a very rare condition that occurs due to loss of soft tissue and cartilage support, can occur due to congenital abnormalities of the larynx and is the sixth leading cause of cancer death worldwide; recognised as one of the most difficult and challenging malignancies to treat [12]. The five-year survival rate for patients with oesophageal cancer is less than 20% [10].

There are three types of stenosis. The first is inflammatory or granulomatous stenosis (Figure 1.1(a)); this is a localised lesion. The second type is the membrane type (Figure 1.1(b)), which consists of a membrane that grows centrifugally and decreases the diameter of the trachea. Both lesions do not change the structure of the trachea. The third type, the so-called stricture (Figure 1.1(c)), is a more complex lesion that modifies the cartilage structure of the trachea; it is a narrowing in one area of the tracheal wall itself. The latter has a more complex treatment and evolution.

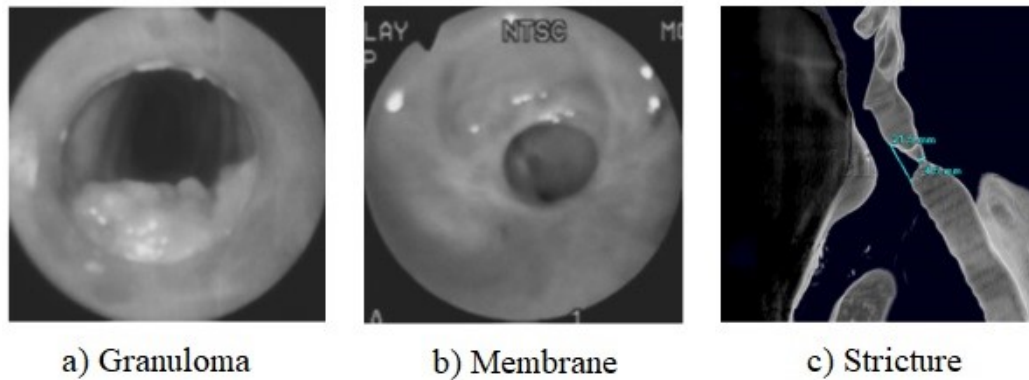


Figure 1. Different types of stenosis.

For patients with inoperable oesophageal malignancies, oesophageal stents offer an effective palliative therapy to allow them to drink and feed orally and swallow saliva. However, there are several alternatives for treating tracheal stenosis. Surgical removal of the affected part is the treatment of choice, especially in benign stenosis, but there are other possibilities such as airway dilatation, electrocautery, argon plasma coagulation, laser ablation, photodynamic therapy, cryotherapy, brachytherapy, or radiotherapy [13] [14] [15] [16].

Typically, a tracheal endoprosthesis needs to be inserted after bronchoscopy. Recently, the treatment of tracheal stenosis has been improved by the technique of tracheobronchial stenting, but stent migration, fibrosis and acute inflammation of the tracheal wall, in-stent restenosis (ISR) and tracheal obstruction have necessitated further clinical intervention in the stented lesion [3].

1.2 Stent

The emergence of stents is a consequence of the introduction of the most common techniques in the field of engineering in support of the world of medicine. In fact, classically, the worlds of medicine and engineering were treated as independent fields of work, with practically unrelated technologies, techniques, and intermediate developments. With the introduction of bioengineering, as result, medical devices have been improved and new

techniques and methodologies have emerged to meet needs that the old techniques could not satisfy, such as stents. The latter were initially created to treat various cardiovascular diseases, but they have now been extended to treat other types of pathologies affecting different conduits of the human body. Their functionality is therefore highly critical and relevant to health. It is precisely cardiovascular diseases that are considered the leading cause of death in the world, and stenting has become truly crucial, with more than 3 million cardiovascular stents being implanted per year [1]. In addition, airway stents have been implanted to treat central airway obstruction, a critical and common problem for 30% of patients with advanced lung cancer [17].

The continuous search for improvement on these devices is strongly justified by the desire to develop models suitable for the treatment of different diseases and to address the limitations that already developed stents have.

1.2.1 Application

A stent is a small wire mesh tube that can be introduced into organs with a lumen (i.e. hollow, such as blood vessels or intestines) in order to support their internal walls. Its use is particularly common in the vascular field, where stents are inserted into arteries that are narrowed or characterised by weakness. This is the case with coronary angioplasty, in which the placement of the stent allows the vessel to remain open while allowing blood flow. The first stent was implanted in a patient in 1986 in France to treat coronary artery disease. Since then, a lot of research has been done on stents, from the different design patterns to the different materials or applications. Nevertheless, ideal stents have not been created yet as complications still exist, and research needs to continue being done. Most stents are made from wire mesh and are permanent. Some are made of fabric. These are called stent grafts and are often used for larger arteries. Others are made of a material that dissolves, being absorbed by the body over

time. They can be coated to ensure slow drug release into the arteries to prevent them from obstruction recurrence.

1.2.2 Sites of application

There are several application sites for stents; therefore, depending on the location, the specific purpose and consequently the geometry and materials of a stent change.

The main application sites will be listed below in a very general way.

- **Blood vessels:** stents treat arteries blockages and restore the blood flow. Depending on the location of the treated artery, stents are distinguished into:
 - Coronary stents: these are the most common stents, and their purpose is to treat the narrowing of coronary arteries usually caused by atherosclerosis.
 - Peripheral stents: these stents include all those implanted in arteries all around the body, commonly in the lower extremities.
 - Carotid stents: these stents could be included in the peripheral ones but given the importance of the treated artery and their transcendence they are grouped separately.
 - Brain stents: these stents main purpose is to treat brain aneurysms by excluding the created bulge from blood circulation.
 - Renal artery stents: similar to the carotid stents and because of the relevance of the renal artery they are again grouped apart from the peripheral.

- **Airways:** stent implantation aims to treat narrowed air ducts and restore the correct air circulation impeded by blockages. Regarding the placement, they can be differentiated into:
 - Tracheal stent
 - Bronchial stent

Both the tracheal and bronchial are implanted to restore the collapsed air flow or to prevent possible obstructions, being the first ones implanted in the trachea and the others in the bronchi.

Of relevance to this study is the tracheobronchial stent. Ideally, a tracheobronchial stent should be easy to insert and remove, provide a sufficient radial force to avoid migrations, possess high compliance and elastic recoverability without material fatigue, be well tolerated without damaging the airway, have optimal biocompatibility in order to avoid a foreign-body reaction, granulation tissue and/or precipitate infection, and, finally, preserve mucociliary clearance of the tracheal epithelium [18] [19] [20].

- **Digestive ducts:** in these passageways, stenting is directed to reimpose the flow of solids and fluids from the mouth to the stomach. These stents are normally placed in the oesophagus, and they are so-called oesophageal stents.
- **Bile ducts:** biliary stenting is intended to relieve the obstructions impeding the correct flow of bile, which in these cases is unable to aid in digestion.
- **Ureters:** ureteral stents are meant to clear obstructed areas of the ureter and restore the circulation of urine from the kidneys to the bladder.

The principal purpose of the current design is to carry out a parametric study, on an animal model, of a new type of customisable stent for the trachea, with the aim of widening the narrow passages. This study is preliminary to the translation in a human model.

1.2.3 Typologies

There are many stent typologies that can be classified based on:

- specific geometry;
- particular use;
- adopted materials.

The following will present different types of stents available in the market, classified by manufacturing material. The advantages and disadvantages of the different stent typologies will also be reported.

1.2.3.1 Metallic stents:

These stents belong to the category of non-biodegradable stents. They have a tubular mesh structure consisting of a thin metal wire. They were first used in 1987 [21] and their use is considered the second revolution in interventional cardiology [22]; indeed, they are widely used in arterial diseases. They are characterised by strong radial strength and good flexibility. However, these powerful mechanical properties are countered by poor long-term interaction with the surrounding tissue. Although metals with good biocompatibility are used in their construction, ensuring low rates of neointimal hyperplasia and stent thrombosis, their presence usually causes complications, such as in-stent restenosis, subacute thrombosis, tissue inflammation, risk of loosening and fracture. Nevertheless, these devices have good biocompatibility and mechanical properties and provide sufficient scaffolding to the target arteries [23].

For malignant oesophageal obstruction, self-expanding metallic stents (SEMS) have been widely used in recent decades [12]. These metal stents exploit the advantages of the mesh structure to self-expand after being inserted into the oesophagus, thus opening the oesophagus occluded by tumour tissue [10]. The mesh structure means that the stent is easily compressed to a small size so that it can be loaded into a stent-release device before being deployed into the

oesophagus [13]. Although the clinical use of these SEMS has grown tremendously in recent decades due to the ease of placement, complications associated with these SEMS have occurred early or late in the procedure. These complications, previously reported, include tumour tissue growth, bleeding, stenosis recurrence, perforation, reflux disease and stent migration into the stomach [14]. One of the causes of these complications is precisely the network structure of the SEMS.

1.2.3.2 Hybrid Stents:

To reduce the complications associated with the long-term presence of metal stents in the body, these have recently been increasingly replaced by silicone-coated metal stents, the drug-eluting stents (DES). These stents have a more complex structure consisting of the same tubular meshwork structure described above, surrounded by a polymer coating containing an anti-proliferative drug around the stent struts. By this mechanism, cell proliferation and thus hyperplasia and stent thrombosis appear to have been eliminated. However, drug release from the polymer coating does not last forever and consequently, these stents may not inhibit restenosis but only delay it [8]. In addition, although partially or fully covered stents may prevent tissue growth, DES increase the rate of migration and other complications. In addition, metal stents occasionally lead to complications such as fistulas or perforations [16] [18]. Given their characteristics, coated stents should be used in patients with malignant stenosis, where the tumour tends to grow in the airways.

1.2.3.3 Plastic Stents

They present a cylindrical shape that provides a domed effect whereby the compressive forces are evenly distributed. Its flexibility facilitates placement and improves tolerance and secretion clearance. Protrusions on the outer surface of

the stent reduce its movement and prevent mucosal ischaemia by limiting contact with the tracheal walls [24].

One of the materials adopted for these stents is silicone. The main advantage of silicone stents is that they can be easily adjusted and removed and can be repositioned and changed as often as necessary. With this type of stent, there is no internal regrowth or adverse mucosal reaction. For instance, Dumon-type silicone stents are designed specifically for the trachea and will be the one used in this study as a term of comparison with the new models to be tested.

There are also commercially self-expanding plastic stents (SEPS), that have been used for the treatment of benign oesophageal conditions, as they have several advantages with respect to standard SEMS: low cost, ease of placement and retrieval, limited local tissue reaction, effectiveness for treating the benign oesophageal condition. However, SEPS have a high overall rate of stent migration and limited use in alleviating dysphagia caused by benign strictures [2]; it is precisely for these reasons that SEMS are preferred.

1.2.3.4 Biodegradable Stents

A newer generation of stents is the Biodegradable Stent (BDS). The scientists noticed that the permanence in the human body of the BMS device was not safe for the patient and for this reason the research went in another direction. BDS is the fourth revolution in interventional cardiology [22]. These devices can support the inner vessel wall for a limited period, of about 4-6 months. After the healing period, the vessel will be healed, and the biodegradable stent will be absorbed and degraded. The use of BDS thus leads to vascular restoration, which is a great advantage because it preserves the physiological integrity of the vessels, positive long-term remodelling and reactive vasomotion [25].

Traditionally used BMS such as stainless steel and titanium can cause after-effects because they remain in situ even after vascular repair. In this regard, BRS

was introduced to overcome these limitations and exhibit some significant advantages, such as complete bioresorption, mechanical flexibility and not producing imaging artefacts in non-invasive image-based diagnostic [26]. However, other problems are associated with their use. Considering their lower stiffness and strength compared to BMS, radial resistance is the main concern for biodegradable stents. Furthermore, non-uniform degradation may lead to thrombosis and remains a problem to be addressed. In addition, dislodgement between the stent and the deformed conduit may occur, causing another obstacle to the proper functioning of stents, and resulting in excessive damage such as migration problems. This can be explained by variations in treated passages between different patients and is a major complication in applications where the treated passage is subject to many movements and reactions, as is the case with airway stents.

These problems of under- and over-sizing could be addressed with customisable stents, but this can be a very costly process, therefore feasible and effective customisation would be required.

1.3 Respiratory System - General

The respiratory apparatus (or respiratory system) is responsible for the uptake of oxygen (O_2) and the elimination of carbon dioxide (CO_2) from cellular anabolism.

Cells continuously require oxygen to carry out metabolic reactions. At the same time, these reactions release carbon dioxide. Excess CO_2 produces acidity that can be toxic to cells, so it must be removed quickly and efficiently. The two systems that contribute to the supply of O_2 and the elimination of CO_2 are the cardiovascular system and the respiratory system. The latter performs a gas exchange (O_2 supply and CO_2 excretion), while the latter carries blood, which transports gases between the lungs and the tissue cells. Failure of one or the other

disrupts homeostasis by causing rapid cell death through oxygen deprivation and accumulation of waste products. In addition to carrying out gas exchange, the respiratory system is involved in blood pH regulation; it has receptors for the sense of smell; it filters inhaled air, produces sound and removes some of the body water and heat in exhaled air [27].

The process of gas exchange in the body, called respiration, consists of three basic parts:

1. Pulmonary ventilation, also simply called respiration, is the mechanical flow of air into the lungs (inhalation or inspiration) and out of the lungs (expiration or exhalation).
2. External respiration is the exchange of gases between the alveoli of the lungs and the blood in the capillaries of the lungs. In this process, the blood flow in the capillaries receives O₂ and delivers CO₂.
3. Internal respiration is the exchange of gases between the blood in the capillaries of the rest of the body and the cells of the tissues. In this process, the blood gives up O₂ and receives CO₂. Metabolic reactions within cells in which O₂ is consumed and CO₂ is produced during ATP synthesis are called cellular respiration.

1.3.1 Anatomy of the respiratory system

The respiratory apparatus of a rabbit is made up of: [28]

- The nose, nasal cavities, sinuses. These are responsible for facilitating the entry and exit of air, filtering it of dust and other foreign particles.
- The larynx is a tube composed of several mobile parts that establish communication between the trachea and the fauces. It is located below the pharynx.
- The trachea, which is a continuation of the larynx and consists of a long tube, the walls of which are reinforced with reddish, elastic, C-shaped

cartilaginous rings. The trachea enters the thorax where it connects with the bronchi.

- The bronchi, which follow the trachea, are the third organ of animal respiration. At the end of its course, the trachea branches into two parts called bronchi, which, after entering the base of the lung, branch in turn into a series of bronchioles that end in the pulmonary vesicle and alveoli.
- The lungs, the last organ of respiration, are made up of two large masses of spongy structure. Their mission is none other than to make breathing possible and, more specifically, to collect oxygen from the air in order to purify the venous blood that reaches the heart. The two lungs are not the same: the right lung is divided into three lobes or portions, while the left lung has only two. Outside air enters the lungs through the bronchi, trachea, larynx and mouth. The lung is merely the oxygen receptor organ, while the mouth, larynx, trachea and bronchi form the conduit that carries air to the lungs.
- The pleura are serous membranes that cover the lungs and support them. Both pleurae retain a serous fluid, the pleural fluid, whose purpose is to facilitate the movement of the lung.

1.3.2 Pulmonary ventilation

Pulmonary ventilation, commonly called respiration, is the process by which gases are exchanged between the atmosphere and the pulmonary alveoli. The flow of air between the lungs and the atmosphere is due to alternating pressure differences that generate contraction and relaxation of the auxiliary muscles of respiration. The magnitude of airflow and the effort required for respiration are also influenced by alveolar surface tension, lung compliance and airway resistance.

Air enters the lungs when the pressure inside the lungs is lower than the atmospheric air pressure and leaves the lungs if the intrapulmonary pressure is higher than the atmospheric pressure.

1.3.3 Inspiration

Inspiration or inhalation is the part of lung ventilation where air enters the lungs. Just before each inspiration, the intrapulmonary air pressure is about equal to atmospheric pressure, or about 760 millimetres of mercury (mmHg) or 1 atmosphere (atm) at sea level. For air to enter the lungs, the pressure in the alveoli must be lower than atmospheric pressure. This is achieved by increasing lung volume.

1.3.4 Exhalation

Exhalation, the process by which air is expelled through the respiratory system, is also due to a pressure gradient, but in this case the pressure in the lungs is greater than atmospheric pressure. Normal expiration during quiet breathing, unlike inspiration, is a passive process because no muscle contractions are involved. Instead, breathing occurs by the elastic rebound of the chest wall and lungs, which naturally tend to contract after stretching. Exhalation becomes active only during forced breathing, such as when playing music on a wind instrument or during physical exercise. In such circumstances, the auxiliary muscles of respiration (abdominals and intercostals) contract, which increases the pressure in the abdomen and thorax.

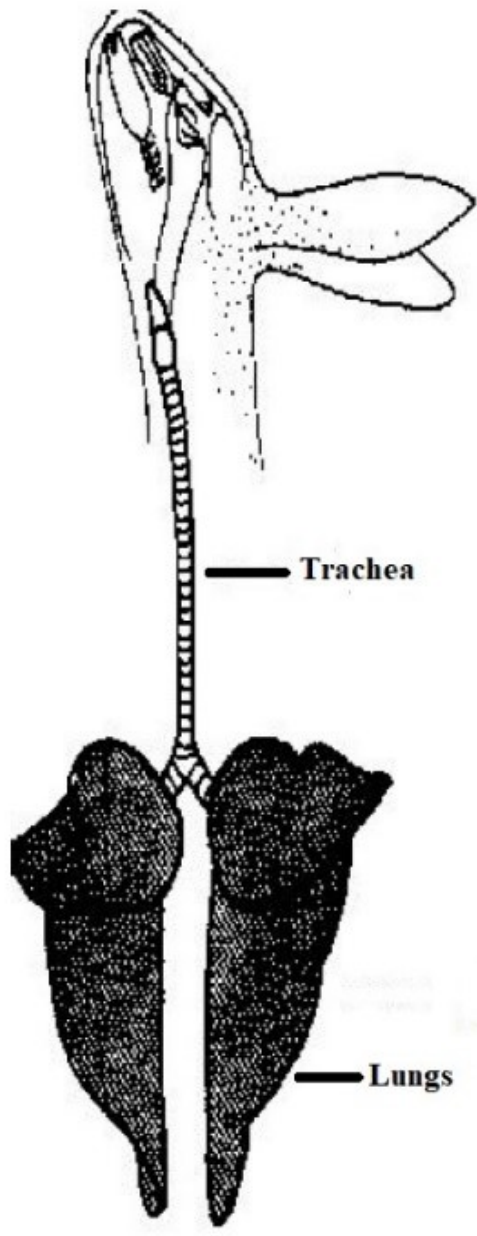


Figure 2. Schematic representation of the rabbit's respiratory system.

CHAPTER 2

Methods

It was necessary to create a model of an animal trachea based on the anatomical information provided in the literature. Similarly, geometries of various stent types were created and appropriately scaled to fit the dimensions of the rabbit trachea. Once the final overall 3D geometric model of the trachea and prosthesis was created, finite element analysis (FEA) served to evaluate the interaction between the biological tissues and the various type of stents, providing truly accurate results. Moreover, this type of analysis is intended to be partially alternative to animal tests, as FEM based models reveal to be a reliable tool to estimate the structural behaviour of biological systems, thus integrating experimental data.

Indeed, because the general aim of this project is to create customisable stents that can be 3D-printed, this methodology allows for a preventive evaluation of the stents' biomechanical behaviour before they are generated.

All 3D geometries of stents and trachea were obtained using SolidWorks. FEM-based analyses were developed using the general-purpose software ANSYS.

2.1 Workflow

SolidWorks was used to create the stent geometry and parameterise it. Indeed, by using parameterisation, the model of the stents can vary by changing specific parameters, allowing their geometry and size to be modified. The models of the three stent types, with the addition of the commercial Dumon stent, were imported into the ANSYS Workbench, for FEA to assess their functionality.

2.2 SolidWorks

SolidWorks is a computer-aided design (CAD) and computer-aided engineering (CAE) programme for solid modelling. The software enables the creation of 2D and 3D geometries. The company was founded in 1993 by the Massachusetts Institute of Technology. The first version of the programme was released in 1995 and now the latest is 'SolidWorks 2021', which is the one used for this work. SolidWorks is a solid modeller that uses a parametric feature-based approach. In fact, it is important to know that parameters refer to constraints whose values define the geometry of the design or assembly. Parameters can be numerical and/or geometric: the former are line length or circle diameters, and the latter are parallel, horizontal, vertical, concentric, tangent, or coincident constraints. By associating one numerical parameter with another using specific relationships, the design idea is captured. This makes it possible to optimise the device according to requirements. With the use of this software, it is possible to specify which parts are to be modified by changing even a single parameter. Features refer to the constituent elements of the part. They are the operations and shapes of which the part is composed. Shape-based features begin with a 2D or 3D sketch of the desired shapes and then these are extruded or filled by adding or reducing material.

In this work, the implemented device measurements are linked to five basic parameters, as will see in the section on stent geometry. By varying the value of

one of them, the desired stent design is actualised and, consequently, the device characteristics meet the requirements arising from its application. For example, in this case, specific devices were made for the trachea model of a rabbit, but the parameterisation used derives from a study made for the human model with the possibility, by varying the parameters, of generating a customised model based on the patient. Once the various models used for this project are set, they are ready to be imported into the ANSYS commercial package for the structural analysis. An advantage of parameterisation is that when a geometric parameter changes in SolidWorks, it will have a consequential effect on the FE model: once the design changes, the computational model will be updated accordingly.

2.3 ANSYS

ANSYS (ANSYS Inc., Canonsburg, PA, USA) is an engineering simulation software based on the finite element method, invented by John Swanson in 1970. In 1993, the founder sold the company, and it has been listed on the Nasdaq since 1996. The industry bought another company, expanding its engineering knowledge in the fields of fluid dynamics, electronic design, and physical analysis. ANSYS software was invented and produced as a finite element analysis programme used for the simulation of engineering problems.

The programme allows the additional creation of structures or machine/electronics components to test strength, toughness, temperature distribution, electromagnetic phenomena, fluid flow, and other characteristics at the simulation level. The advantage of a FEM software is to allow the evaluation of the performance of a system under different conditions, as a preliminary phase, before creating physical prototypes or developing destructive experimental tests. In this work project, the simulations are realised with Ansys Workbench, one of the company's most popular software.

2.4 ANSYS Workbench

The ANSYS Workbench, together with the Workbench projects and tabs, provides a unified working environment for developing and managing a variety of CAE information, Figure 3. Moreover, the ANSYS Workbench environment is an intuitive up-front FEA tool that is used in connection with CAD systems and/or Design-Modelers.

The steps of pre-processing, analysis and results are described in the following:

- Engineering Data
- Geometry
- Model
- Setup
- Solution
- Results

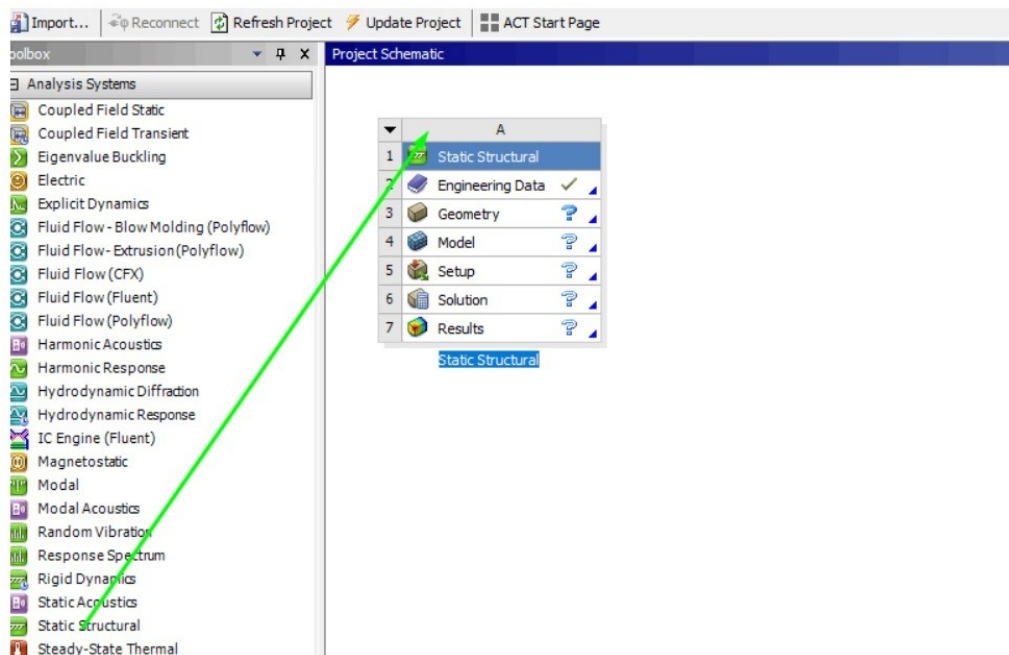


Figure 3. ANSYS Workbench blocks diagram.

Engineering Data is the first section in the process of creating the model and is important for defining material characteristics. By opening this interface, material parameters can be defined. In addition, it is possible to define specific

mechanical behaviour and other material characteristics of interest. This technical data section presents an extensive list of different materials. Figure 4 shows the main window presenting the mechanical behaviour that can be selected on the left. Choosing, for example, 'isotropic elasticity' a second window will be opened, in which it is possible to fill the fields with appropriate values. In the upper part and on the right of the main material menu, the stress-strain curve with the set parameters is shown.

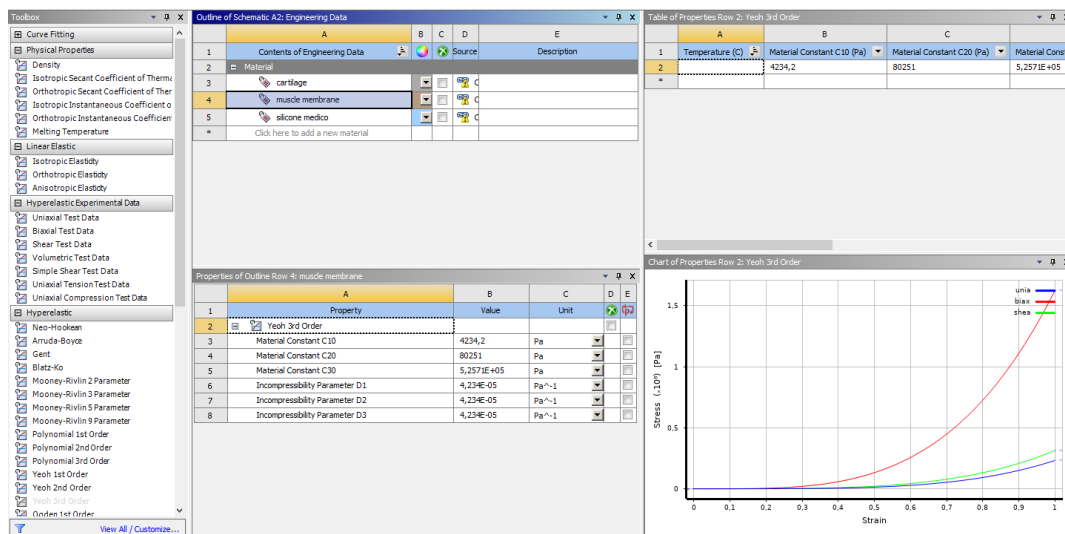


Figure 4. Engineering Data section.

Geometry of the device can be implemented directly in the Workbench or can be imported from other software, such as SolidWorks. This method of importing geometry from an external software to ANSYS does not allow the modification of a loaded geometry. All the geometric features must be defined in the source software and then automatically imported into the so called Geometry section of ANSYS. For this reason, once a geometry has been updated, a check must always be made that all parts have been loaded correctly and that the measurements correspond with the source file. The capability of linking the two software provides the advantage of using advanced software to create the geometry. This makes it possible to overcome the limits of ANSYS, which is provided with a reduced number of functionalities for the creation of geometry. A further

advantage is that the import phase of the geometric model is not time-consuming, as once the two software are linked, a change in the source geometry is automatically considered in the final model.

Model is the main body, where the creation of the model occurs, and it is further subdivided into subsections. As first step, the reference material is assigned to each component of the geometry. The software has a default global coordinate system that can be changed if needed. It is also possible to create additional reference systems of cartesian or cylindrical type.

The next step is dedicated to defining contact regions by assigning to each pair of contact surfaces the most suitable type of interaction properties. The software provides a wide choice of contact types.

Once the contact regions have been defined, it is possible to create the mesh of each geometric feature. The meshing is made after the contact regions have been defined because depending on the type of contact, the software creates a specific mesh for each pair of contact regions. The software provides different methods for creating the mesh as well as various types of finite elements, such as linear tetrahedral elements or hexahedral elements. This phase is strategic in influencing the results. Indeed, the choice of the number of elements requires careful analysis to balance the analysis's computational cost and the accuracy of results.

Setup defines the various boundary conditions and applied loads. To analyse the behaviour of a particular system under an imposed system of forces or displacements, all parameters must be set.

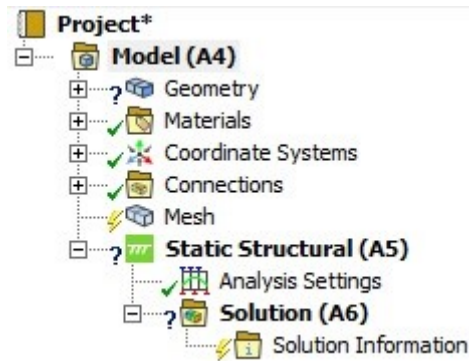


Figure 5. ANSYS Mechanical blocks diagram.

Solution and Results in simulation test processes allow to understand how the device reacts to the imposed conditions. In the solution part, the user must select what is important to check the coordinate system in which he wants to see the solution, in which part of the instrument to observe the results, the observation time, and which variable is to be exported.

The software offers the possibility of displaying several different characteristics and for each of them provides numerical data, a visual overview in the form of a movie, and the maximum, minimum and average values measured. In addition, all data can be downloaded and automatically the software prepares a written report, where all parameters and solution methods used to obtain the results are included. In addition, the prepared data and configuration can be saved in the programme. The visual part, because it is immediately clear what the problems are in the configuration, where the device has higher voltages and how to modify the simulation setup, is essential.

2.5 MATLAB

Version R2021b of MATLAB software was used to graph some of the results obtained from the analysis. MATLAB is a programming and numerical calculation platform used by millions of engineers and scientists for analysing data, developing algorithms, and creating models. Using this software, it was

possible to compare the results of the analysis of the different models to have an overall view and a term of comparison of the stents considered.

Materials

2.5 Materials

Initially, the material used for this project was medical silicone. However, different polymers can be adopted in medicine, taking advantage of their specific properties [29]. In general, polymeric stents are made of silicone and only a few contain copolymers and additional additives, although increasingly biocompatible and possibly biodegradable materials are being investigated. In fact, once silicone, the material proposed in the study by [30], has been used, other materials such as polydimethylsiloxane (PDMS) and polyvinyl alcohol (PVA) have been used. Silicon and polymers are the typical materials used for microdevices fabrication. Silicon, because of its thermal conductivity and the availability of advanced fabrication technologies and polymers, because of its low cost, optical transparency and flexibility. Compared to silicon, PDMS turns out to be the most promising elastomer, because silicone has a high manufacturing cost, requires greater labour intensity and is rigid in nature. PDMS presents a hyperelastic behaviour, which is the ability of a material to undergo large deformations before rupture [31]. This characteristic is also found in biological tissues and, for that reason, PDMS can be a well-suited material to mimic the trachea tissues [32].

However, the material used to produce the stent must have good resistance to deformation while inserted into the bronchoscope and then, once opened within the trachea or bronchi, must be able to adapt to the physiological activities of the respiratory system [33].

2.5.1 Tracheal tissue

To correctly represent the properties of rabbit tracheal tissue, a model obtained from empirical testing on rabbit tissue, already studied in the literature has been employed [34]. According to this reference, the collagen fibres run randomly because no preferential orientations were observed in the cartilage rings. Therefore, an isotropic material model can be chosen to reproduce the behaviour of the tissue. Moreover, due to the small tensile stresses acting on the rabbit trachea, the muscular membrane can be modelled as isotropic, too.

In the literature there is a hyperplastic model that represent both the cartilage and the muscular membrane, with the Demiray strain energy density function $W = D_1[\exp(D_2(\bar{I}1 - 3)) - 1] + U(J)$ employed to approximate the experimental results. In this function $\bar{I}1$ is the first invariant of the deviatoric right Cauchy–Green tensor $C = J^{-2/3}F^T F$, $J = \det(F)$ is the Jacobian, F is the standard deformation gradient, U is the volumetric energy function and D_1 , D_2 are material constants [34]. However, this model was used specifically for the analysis performed with the software Adina R&D (Bentley Group) [35]. On the contrary, the simulations of the present study were carried out using Ansys, that employs other models for hyperelastic materials. Ansys adopts a Yeoh's third-order model, whose strain energy density function is:

$$W(\bar{I}1, J) = \sum_{i=1}^3 C_{i0}(\bar{I}1 - 3)^i + \sum_{k=1}^3 \frac{1}{d_k} (J - 1)^{2k}$$

The coefficients to be used in this model were found in the literature from previous experimental set-ups on rabbit biological tissues performed at the University of Zaragoza [35]. In particular, the tracheal muscle sample was submitted to tensile tests obtaining experimental curves later fitted using both Demiray and Yeoh material models. The model coefficients of the Yeoh model can be found in Table 2. Notice that $d_1 = d_2 = d_3$

| Parameters | C_{10} (kPa) | C_{20} (kPa) | C_{30} (kPa) | d (kPa ⁻¹) |
|-------------------|----------------|----------------|----------------|--------------------------|
| Cartilage | 518.6 | 17954.2 | 24.3 | 0.052 |
| Muscular membrane | 4.2 | 80.3 | 525.7 | 0.042 |

Table 1. Obtained parameters from adjusting the parameters of Table 9 to a 3rd-order hyperelastic Yeoh model. C_{10} , C_{20} and C_{30} represent the material constants while d is the incompressibility parameter.

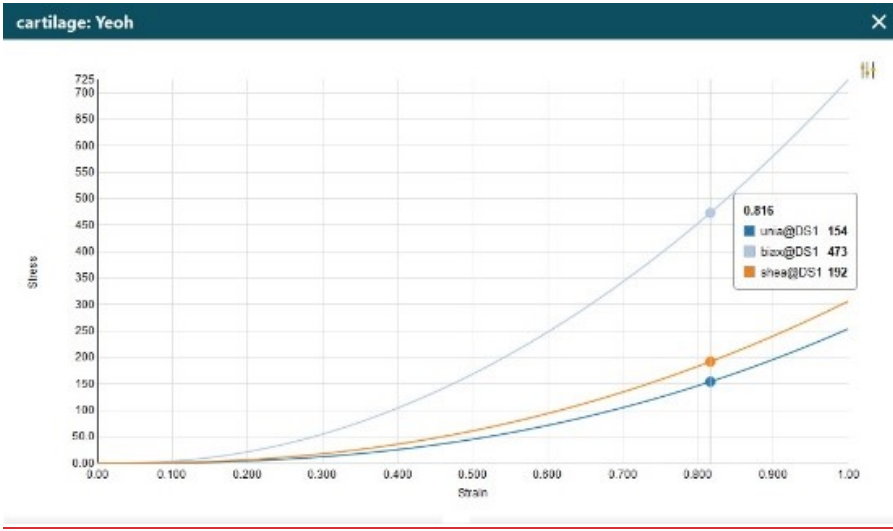


Figure 6. Stress-Strain graph of cartilage tissue.

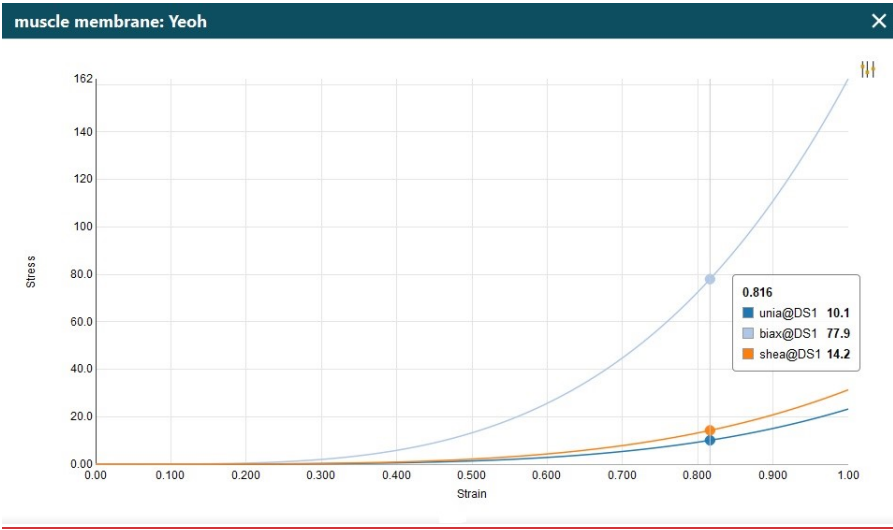


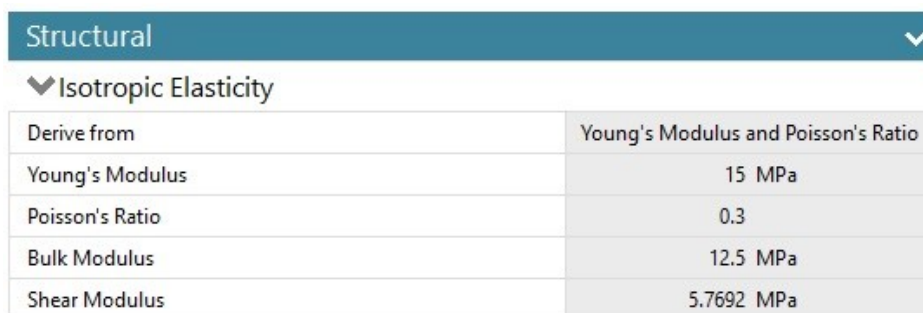
Figure 7. Stress-Strain graph of muscle membrane tissue.

2.5.2 Stent Material

The three samples produced for the animal experiments conducted by the University of Zaragoza were produced by the 3D printing technique, using medical silicone. This 3D printing technique allows objects to be made from a solid filament, which is then melted and deposited layer by layer by the 3D printer head. The materials used are thermoplastic polymers such as medical silicone. In addition to silicone, PDMS and PVA were also used in the FE analyses. These new-generation materials, which allow for better biocompatibility, were included in the analyses to biomechanically assess the device at zero time of application inside the trachea.

Medical Silicone:

Medical silicone has a modulus of elasticity of 15 ± 0.4 MPa, obtained after an analysis of the material properties at AIN (Asociación de la Industria Navarra, Pamplona, Spain). In particular, the stress-strain curve was obtained by means of a tensile test. The curve obtained showed a linear elastic region up to a strain of about 37% [34].



| Derive from | Young's Modulus and Poisson's Ratio |
|-----------------|-------------------------------------|
| Young's Modulus | 15 MPa |
| Poisson's Ratio | 0.3 |
| Bulk Modulus | 12.5 MPa |
| Shear Modulus | 5.7692 MPa |

Figure 8. Mechanical proprieties of medical silicon.

Polydimethylsiloxane

Polydimethylsiloxane (PDMS) is an elastomeric polymer with excellent mechanical properties, which makes it well-suited for several engineering applications. Due to its biocompatibility, PDMS can be used as material for biomedical purposes.

Two different compositions of PDMS were used: PDMS 5:1 and PDMS 10:1. These compositions have different base/agent ratios, which mean different degrees of cross-linking of the polymer chains. The lower the degree of PDMS cross-linking, the softer PDMS is. The values of Young's modulus and the Poisson's coefficient considered for the isotropic elasticity were obtained from the literature [36], for PDMS 5:1 is 3.59 MPa, while for PDMS 10:1 is 2.66 MPa, with a Poisson's coefficient of 0.49.

Polyvinyl alcohol

Polyvinyl alcohol (PVA) hydrogel is a biodegradable synthetic polymer which is usually used as scaffolds for tissue engineering due to its biocompatibility. It was selected to mimic the behaviour of the trachea tissue due to its suitable compressive stiffness and large water content [37]. To improve biodegradation properties, partial oxidation of PVA is performed using different oxidizing agents, such as potassium permanganate, bromine, and iodine [38].

PVA and a partial oxidation of PVA, oxidised with the potassium permanganate (KMnO₄), were investigated and their elastic moduli were extrapolated from tension-strain curves (Figure #) studied in previous works [38].

Since the elastic modulus is defined as $E = \sigma/\varepsilon$, the ε strain has to be known. So, ε is calculated from a model of a healthy trachea subjected to normal pressure at the inner surface of 200Pa, the maximum pressure in a normal rabbit breathing cycle and a change in diameter of approximately 2.5% was found. Therefore, secant moduli of elasticity were extrapolated from the respective stress-strain

curves considering the VC value of deformation. Since the stress-strain profile in this section is almost linear, the assumption of linear elastic material was made, assuming elastic modulus equal to the secant modulus of elasticity. As for silicon and PDMS, an isotropic elasticity was considered. Respectively for PVA and OxPVA_KMnO₄ the elastic moduli are 0.229 MPa and 0.06 MPa. Furthermore, considering the quasi-incompressibility of the material, a Poisson's coefficient of 0.49 was considered.

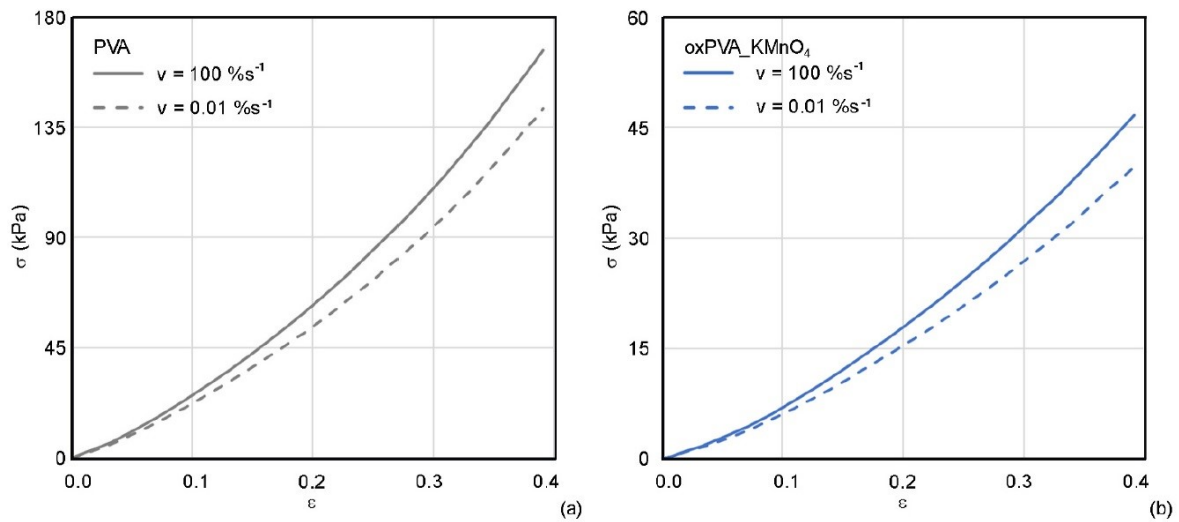


Figure 9. Data reported as Cauchy stress σ vs. nominal strain ϵ for a) PVA and b) oxPVAKMnO₄

2.6 Geometry

2.6.1 Geometry of the trachea

A simplified rabbit trachea model was defined. In particular, a section of the trachea was defined as a cylinder with two distinct tissues: cartilage and muscle. In Figure 10, the regions corresponding to the two tissues can be seen. The green part is the cartilage, forming incomplete rings along the length of the trachea; the purple part is the muscle filling the left region and closing the circumference. The cartilage area is 3 mm wide, while the muscle area is 2 mm wide. The muscle area that runs longitudinally along the trachea is 2.5 millimetres wide. Overall,

the trachea model defines a cylinder of 5.5 millimetres in diameter with a wall thickness of 0.8 millimetres.

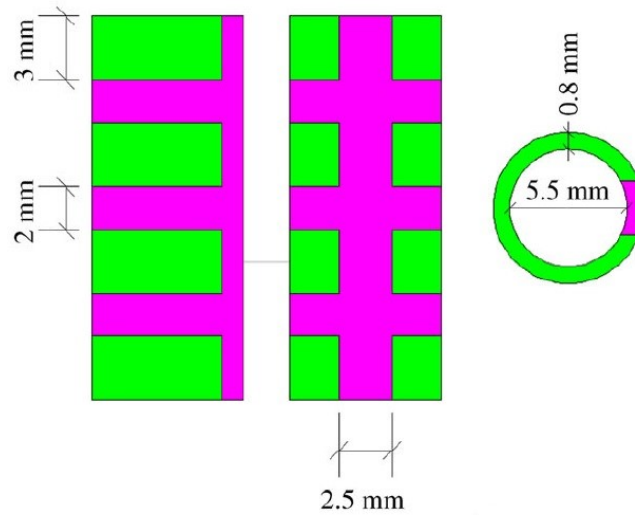


Figure 10. Healthy modelled trachea [34].

Moreover, knowing that the stents were made in such a way as to restore the actual lumen of a healthy trachea, they have a slightly larger outer diameter than the inner diameter of the trachea, consequently, as can be seen in Figure 11, it was simulated the widening of the trachea in the central part as a result of the presence of a stent.

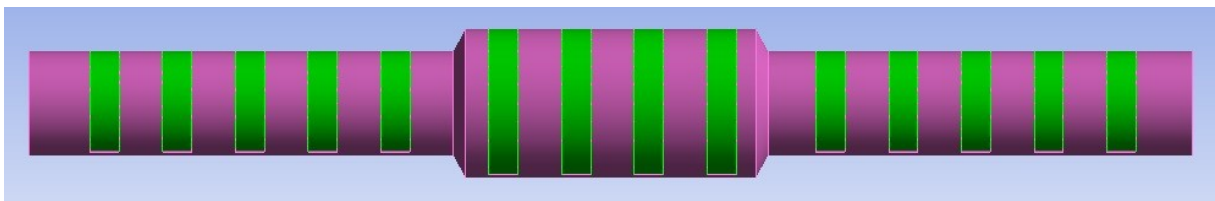


Figure 11. Model of stenosed trachea with stent inserted.

2.6.2 Geometry of the stent

For this research study, a scaled version of the well-known Dumon prosthesis was used as a comparison term for validating the results obtained with the new stent models proposed in the study [30]. The version of the commercial prosthesis was scaled to a reasonable size to fit in the rabbit trachea model, without losing the basic characteristics of the prosthesis. In fact, it was decided to maintain the same internal diameter as the new prototypes and a thickness typical of Dumon's prosthesis [39]. A representation of a commercial version of the Dumon stent is shown in Figure 12.



Figure 12. Commercial Dumon's stent [39].

The new stents were designed with a tubular shape to replicate the classic shape of a commercial prosthesis. A basic CAD model, created with Solidworks software, is shown in Figure 15. The outer part of the tube was designed with a reinforcing structure, similar to typical X-shaped metal stents. Zurita-Gabasa et al. [29] developed the parameterisation of the device geometry to study the effect of each individual feature on the mechanical properties. By modulating the different parameters, it is possible to adjust the redundancy, radial compliance, and mechanical strength of the stent. The basic tube resembles Dumon's commercial stent [39]. The external skewed fibres that reinforce the base cylinder cover only a percentage of the cylinder's outer surface, gradually

reducing their thickness until they reach the outer surface of the base cylinder, as Figure 13 shows. Unlike the Dumon prosthesis, but similar to the metallic mesh stent, the new prototype has an innovative design whose cross-section has a non-homogeneous thickness that favours varying stiffness along the radius. This is intended to simulate the behaviour of the trachea during the physiological manoeuvres of forced breathing, coughing, and swallowing. The trachea, composed of a transverse muscular membrane and stiffer rings of cartilage, dilates and collapses during breathing and coughing, widening, and reducing its diameter. Particularly during coughing, the muscle membrane deforms considerably.

For this reason, the side of the prosthesis that corresponds to the membrane is designed without fibres. Therefore, as can be seen in Figure 13, the fibres cover only a portion of the outer surface of the prosthesis.

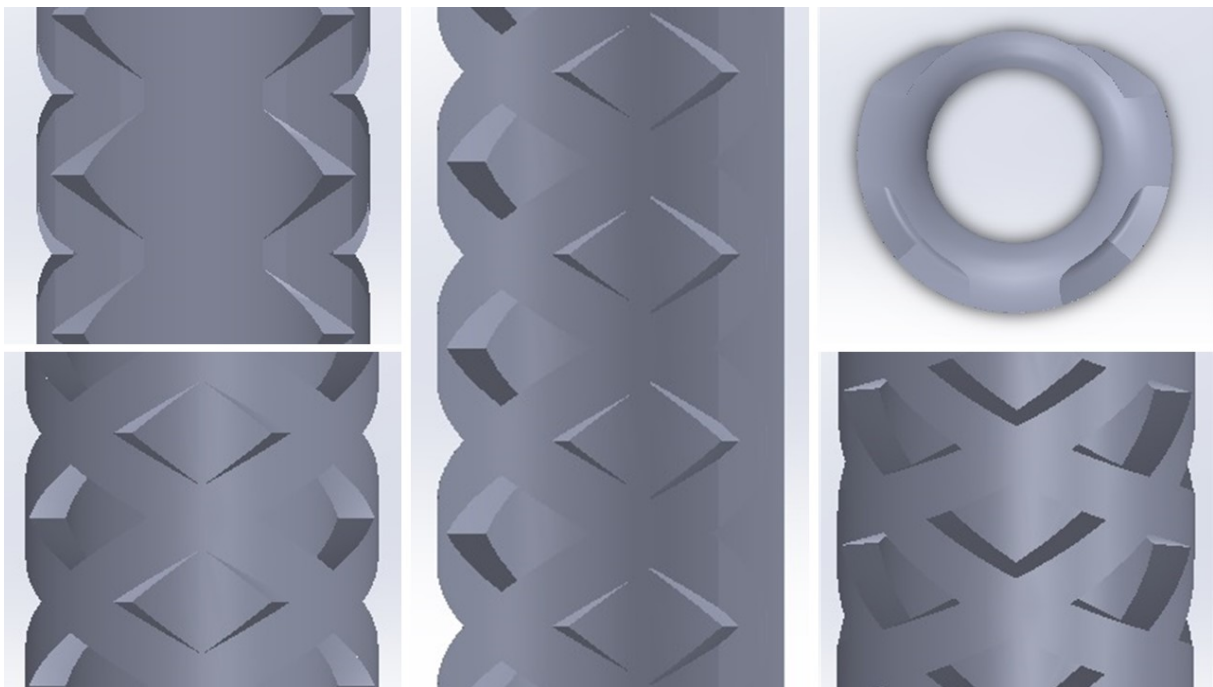


Figure 13. Different perspectives of stent's baseline geometry.

In the study by Zurita-Gabasa et al. [30], the parameterization of the model of this new prototype was implemented. The shape of the fibres that support the

outer surface of the prototype is governed by their number in the longitudinal (n_L) and radial (n_R) directions. Looking at Equation 1 it can be appreciated that an increase in the number of cells in the longitudinal direction favours a smaller α pitch angle, while an increase in the number of cells in the circumferential direction favours a larger α pitch angle (see Figure 14 a)). Furthermore, as can be seen from Figure 16, with pitch angles less than 45° the shape of the cells is a rhombus oriented circumferentially around the outer surface of the prosthesis. On the contrary, with pitch angles greater than 45° , on the other hand, the cell shape is a rhombus oriented longitudinally. The pitch angle can be calculated as:

$$\alpha = \text{atan} \left(\frac{L/n_L}{p(2\pi R)/n_R} \right)$$

where L is the length of the prosthesis, n_L is the number of cells in the longitudinal direction, p is the percentage of the outer surface of the fibre-reinforced prosthesis, and R is the inner radius of the prosthesis and n_R is the number of cells in the radial direction. The parameter p governs the extent of the fibres around the outer surface of the tube and, consequently, the width of the reinforcement region and the width of the fibre-free region of the prosthesis. The radius R and length L of the stent are parameters that can be adapted to obtain a patient-specific stent. Based on this parameterisation, it was possible to produce the three prototypes analysed in this thesis work, to study the interaction between the prosthesis and tracheal tissue in the rabbit animal model. Table 3 shows the parameters used to realise the stent models, corresponding to Figure 15.

| Stent type | n_L | n_R | α [°] | L [mm] | p [%] | R [mm] |
|------------|-------|-------|--------------|--------|-------|--------|
| #1 | 6 | 3 | 36 | 20 | 87.5 | 2.75 |
| #2 | 4 | 3 | 45 | 20 | 87.5 | 2.75 |
| #3 | 3 | 3 | 61 | 20 | 87.5 | 2.75 |

Table 3. Parameters of different stents.

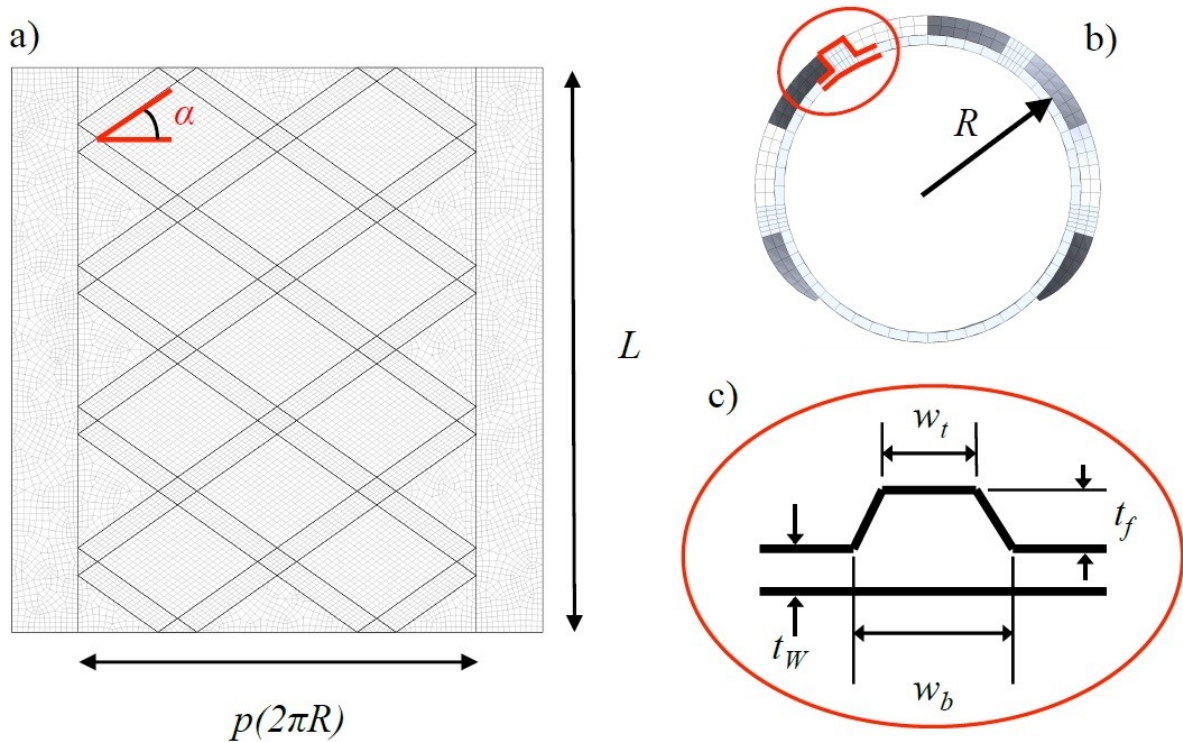


Figure 14. Parametrization of the tracheobronchial stent prototype: (a) unwrapped geometry, (b) top section of the tubular configuration and (c) detail of the stent fibre [30].

The dimensions of the fibres are parameterised. The thickness of the stent is represented by t_w and that of the fibres by t_f . Furthermore, the bottom and top fibre width are represented by w_b and w_t in Figure 14 c). Figure 14 b) shows that the fibre thickness gradually decreases (see also Figure 13). This thickness has biomechanical relevance since it is known that the roundoff of the edges of the whole geometry reduces tissue damage. For the purposes of the numerical simulations, the thickness t_w was considered constant and with a minimum value of 0.8 mm to allow the prosthesis to be fabricated using 3D printing. The parameters t_f , w_b , and w_t were considered constant with values of 0.8mm, 0.8mm and 0.75mm respectively.



Figure 15. Three different types of stents.

2.6.3 Assembly

The figure 16 shows the assembly of the two components of the model (trachea and prosthesis) obtained with Solidworks.

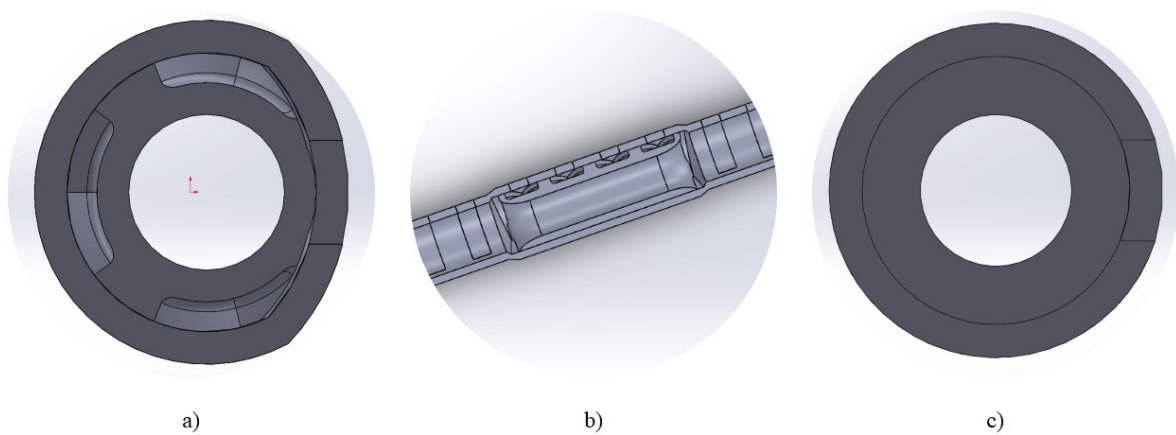


Figure 16. a) Transversal section of stent #2, b) Longitudinal section of stent #2, c) Transversal section of commercial Dumon's stent.

2.7 Meshing

Meshing was performed using hexahedral or tetrahedral, based on geometric complexity. It was preferred to use hexahedral elements, as they facilitate convergence compared to tetrahedral elements. Nevertheless, tetrahedra fit complex geometries quite well compared hexahedra, so they were chosen where the geometry presented discontinuities. However, due to the presence of non-linearity and large deformations associated with hyperelastic fabrics, hexahedral meshes are chosen to ensure convergence. The software allows the elements to be created automatically from the surfaces of the geometry, and due to the complexity of the geometry of the muscular part of the trachea in some places, it is easier to create the mesh with tetrahedral elements. For cartilage rings with a more regular and symmetrical geometry, it was possible to create hexahedral-type elements.

All the meshes of the different models were made in a similar way. In places where greater calculation accuracy is required, for example where there is a diameter discontinuity along the surface of the trachea, the mesh has a higher density by increasing it a little more in the dividing lines of the different areas, to approximate the actual geometry as closely as possible and make fewer errors when performing the calculations. On the other hand, in areas less relevant to the calculation, such as those further from the stent, the mesh density decreases to speed up the calculation.

Once the geometry has been introduced into the programme, we proceed to set up the mesh that will generate the three-dimensional solid elements within it. In this case, once the geometry has been introduced, the programme creates three groups, one for the muscle, one collecting all the cartilage rings and finally one for the stent.

The computational cost will affect the choice of element size, as choosing very small elements will mean an exorbitant amount of time to complete the simulations. A compromise is therefore necessary and reasonable.

To this end, using the face sizing function in the mesh section of ANSYS, it was set that the radial surfaces, i.e. the contact surfaces, of the various components belonging to the trachea and the cartilage rings had a maximum element size of 0.3 mm, as the thickness is 0.8 mm. For the outer and inner surfaces an element size of 0.8 mm was established, as the width of the cartilage rings is 2 mm and that of the muscular part 3 mm. The only difference between the muscle part and the cartilage rings is due to the fact that the programme has created a mesh with hexahedral elements for the cartilage elements, while the muscle part is composed of tetrahedral elements.

For the stent elements, the body size function was used with a maximum element size of 0.5 mm and 0.1 mm, respectively, for the commercial and the new prototypes, which also have ribs on the outer surface. Figure 17 shows a representation of different geometry meshes.

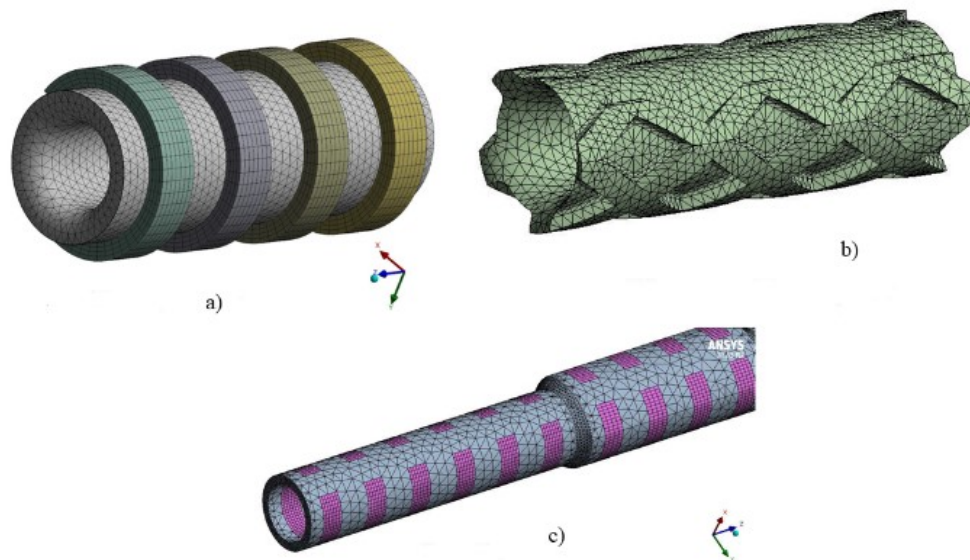


Figure 17. Geometry meshes: a) Refer to the commercial Dumon's stent with the cartilage rings, b) Refer to the type #3 stent, and c) Refer to the affected trachea.

2.7 Boundary Conditions

The setting of boundary conditions is a very important step in the computational process. Before applying the load, some boundary conditions must be set on the component to avoid rigid body motion. This is a very critical step because the correct number of constraints must be specified. If there are fewer constraints than necessary, the system will be under-constrained, and the solution will not converge. However, if the constraints are too large, the system may be incompatible, and a solution cannot be obtained.

2.7.1 Fixed Support

Initially, fixed support conditions were provided for the end transversal sections of the trachea, which represent the attachment to the tissues upstream and downstream of the region considered. This support prevents a selected geometric or mesh entity from moving or deforming. Figure 18 shows one of the two fixed faces.

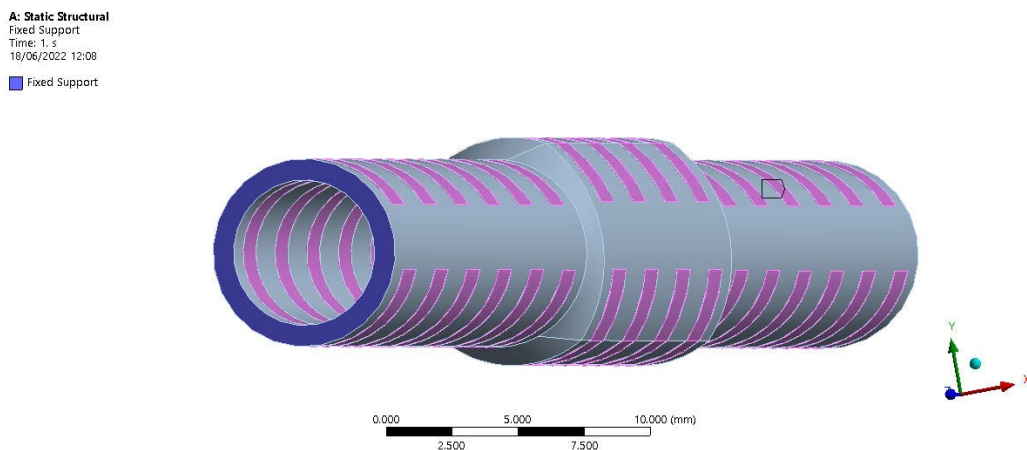


Figure 18. Fixed supports.

2.7.2 Elastic Support

In general, elastic support defines an elastic foundation between the selected faces of a part or assembly and the ground. The elastic support is based on foundation stiffness, which is defined as the pressure required to produce a unit normal deflection of the foundation. Elastic support applies flexible frictionless support to a face. This type of support was applied to all external surfaces of the model to simulate the external environment surrounding the trachea. In fact, the organ inside the human body is in contact with the various tissues that surround it and therefore create a certain amount of resistance. In the literature, stiffness values are not mentioned for this propose, therefore a value of 0.0001 N/mm^3 is chosen to not affect the result of the analysis.

C: PDMS 10:1
Elastic Support 2
Time: 0,26 s
06/11/2022 19:07
Elastic Support 2: $1, \text{e-}004 \text{ N/mm}^3$

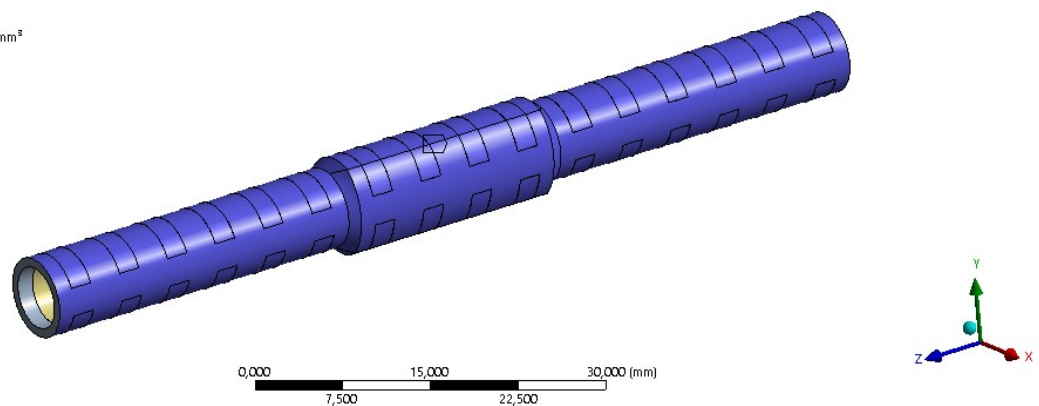


Figure 19. Elastic support.

2.7.3 Contact

Contact pairs must be defined in geometries. The software ANSYS provides point-to-surface and surface-to-surface contact types. In this specific case, surface-to-surface was used. For this contact choice, both the master and the slave surfaces must be determined. Generally, a convex surface is chosen as the master surface and the concave surface as slave. In addition, a large surface is chosen as slave when the size of one body in contact is very small compared to

that of another. Master and slave surfaces are assigned for each pair between the stent and the tissue. In the case of the trachea, there is a pair of contact with the stent for each of the cartilage rings and one for the membrane. In all of them, the stent is selected as the slave body and the tissue as the master body for the same reasoning as already given (Figure 20).

The surfaces in contact between cartilage rings and muscle tissue were considered glued, which means that they are considered as a single surface, so no sliding or separation between faces is allowed. Instead, to establish the interaction between the stent and the tracheal tissue, an ideal frictionless contact between the two was chosen. This type of contact is defined by ANSYS and treats differently both the normal and contact forces. In the normal direction, the surfaces can separate from each other, but cannot penetrate into each other, whereas in the tangential direction, the surfaces can slide over each other without any restriction.

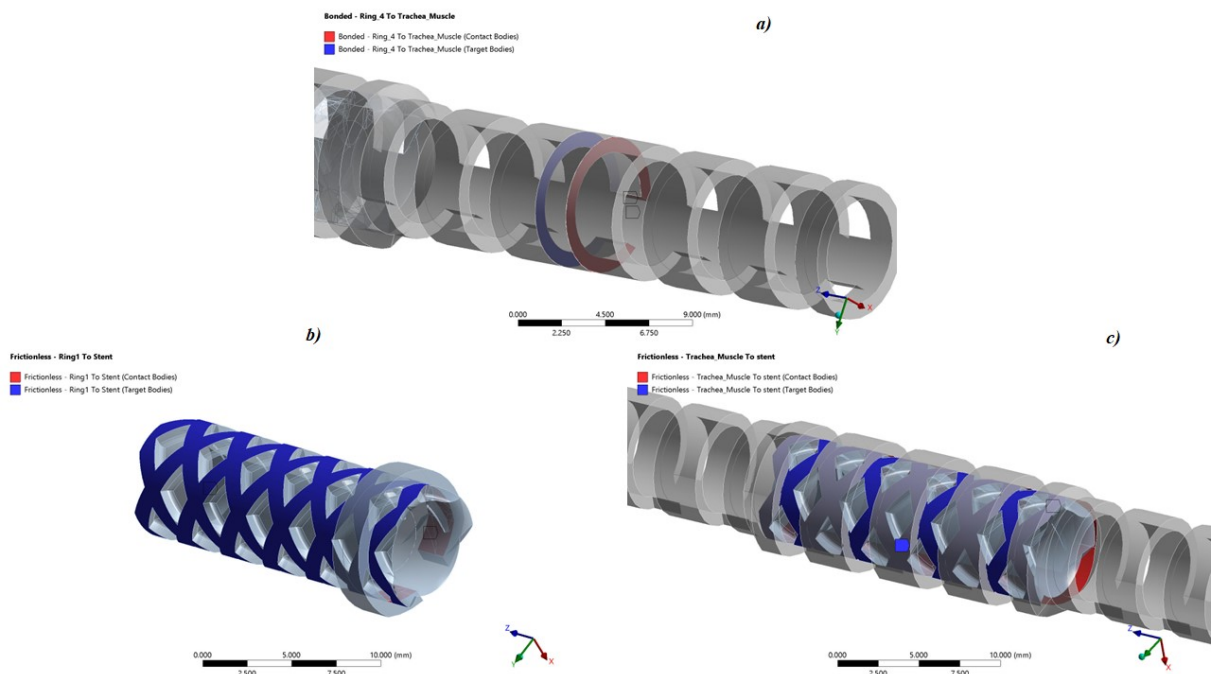


Figure 20. a) Bounded contact between the radial surfaces of cartilage rings with muscular tissue, b) The frictionless contact between the inner surface of cartilage rings with the device's external surface, c) The frictionless contact between the inner surface of muscle tissue with the device's external surface.

2.8 Load

To simulate the inhalation and exhalation of a rabbit's breath, it was adopted a sinusoidal function, in time, with a duration of one second and an amplitude of 200 Pa. According to the data provided by the Zaragoza University of Zaragoza, during breathing, a rabbit exerts a pressure between 1 and 2 cm H₂O, corresponding to a value between 98 and 196 Pa. In this case, a maximum pressure of 200 Pa was applied to the inner face of the trachea and the stent. The rabbit's breathing was dropped by spirometry performed on the rabbit by means of the Datex Ohmeda 7100 anaesthetic machine. These pressure data can be seen in Figure 21.

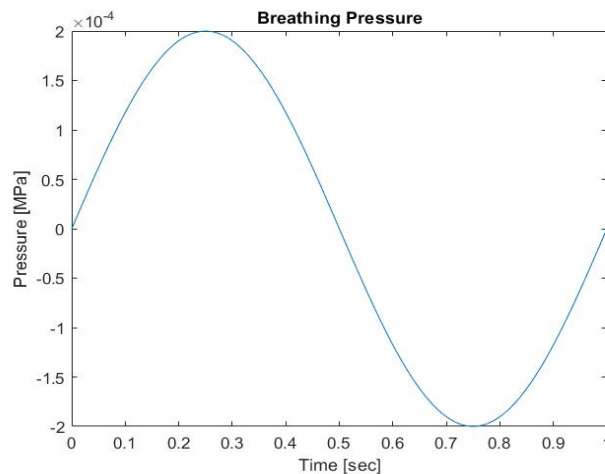


Figure 21. Sinus-shaped time-varying of rabbit breathing.

A: Static Structural
Pressure
Time: 0,25 s
20/06/2022 10:26
■ Pressure: 2.e-004 MPa

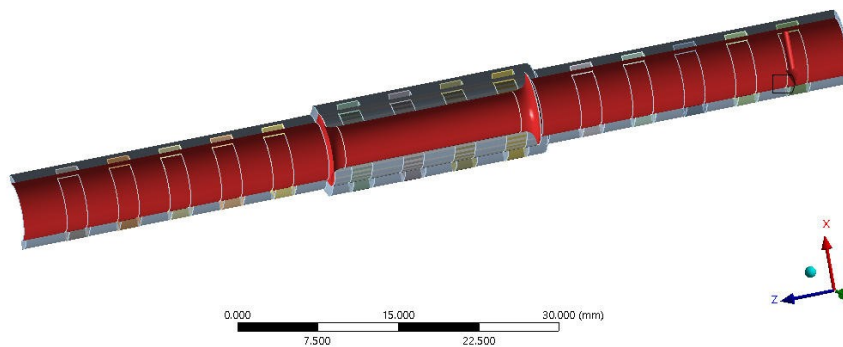


Figure 22. Pressure application sites

CHAPTER 3

Results

In the following paragraphs, the comparison between the mechanical behaviour of the three new-generation tracheobronchial stents realized in silicone and the Dumon commercial stent is reported. Moreover, the same model with alternative materials was investigated to better mimic the mechanical behaviour of the biological tissues of the trachea. Finally, to study the mechanical differences between animal and human prostheses, an analytical estimation of the radial stiffness is proposed. Despite the radius of the human trachea is larger compared to the rabbit trachea, the thickness of the stent is maintained equal between the two devices, because the 3D printing procedure at disposal does not allow to go below the set thickness value.

3.1 Deformation stent results

First, the field of displacement in the x direction was chosen to be investigated as the directional displacement of the numerical simulations. The Figure 23 shows the cross section of a model of a healthy trachea (Figure 23 a), c)) and the model of a trachea with implanted stent #2 (Figure 23 b), d)); the latter was used for the representation as no appreciable differences were found between the simulations with the other stent types, #1 and #3. The Figure 23 represents the directional displacement amplified twenty-fold so that the variations can be better appreciated.

The sections at time points to the peak of positive and negative pressure on the inner surfaces are considered. These time points correspond to the inhalation and exhalation phases, i.e. 0.25 and 0.75 seconds in the breathing cycle.

As expected, in the healthy trachea the cartilage rings and the muscular tissue are stretched in the inhalation phase, whereas they are shortened in the exhalation phase. Nevertheless, during the breathing cycle, the trachea model with implanted stent shows that the tissues in contact with the stent are not significantly involved in the deformation as the stent is largely stiff and develops almost no deformation.

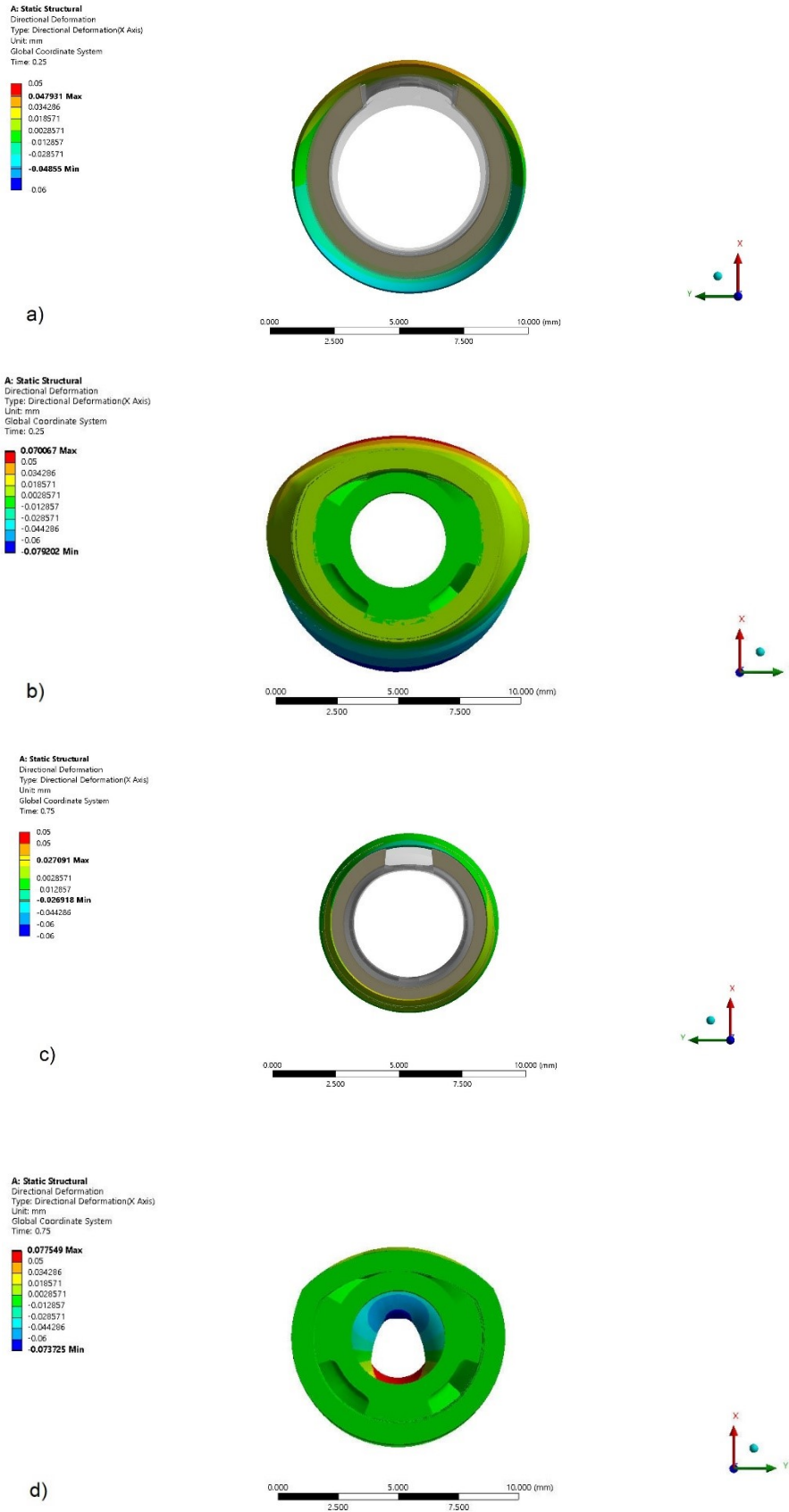


Figure 23. Field of displacement in the x direction (mm) of transversal section during the inhalation phase of a) healthy trachea and b) trachea with stent implanted, and during the exhalation phase of c) healthy trachea and d) trachea with stent implanted.

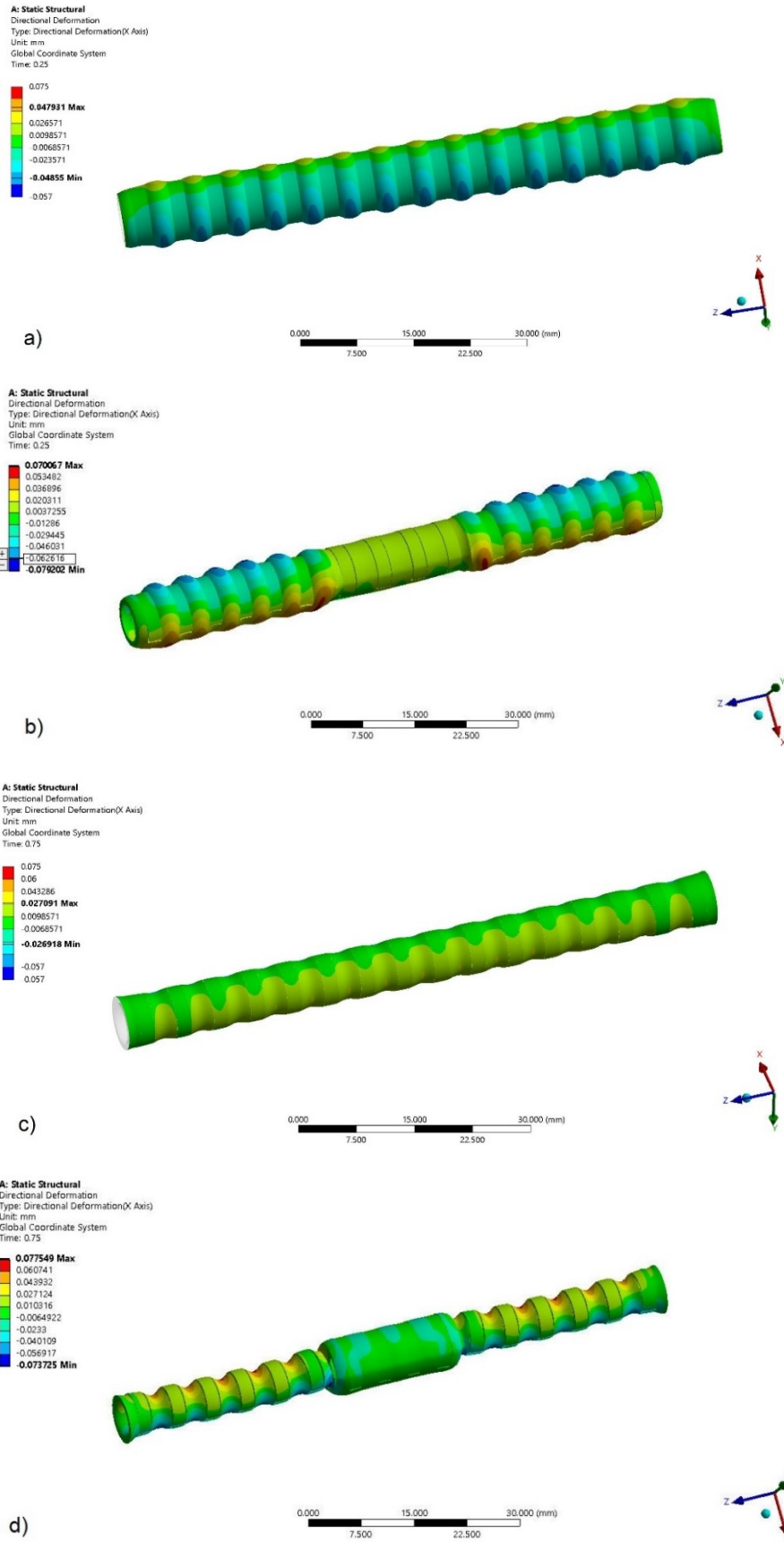


Figure 24. Field of displacement in the x direction (mm) during the inhalation phase of a) healthy trachea and b) trachea with stent implanted, and during the exhalation phase of c) healthy trachea and d) trachea with stent implanted.

Figure 24 represents a general view of the models previously commented. It can be appreciated how the muscular part experiences greater deformation than the cartilage rings.

The field of displacement in the x direction takes similar values for the different models, therefore, to better understand which stent was stiffer the change in the internal diameter of the stent was detected. The graph of Figure 25 shows how the diameter of the different stents changes over time in the breathing cycle. The graph shows variations in the diameter in the order of 10^{-4} mm, which are essentially insignificant for this application assessment. However, it was observed that the new generation stents are less stiff than the commercial.

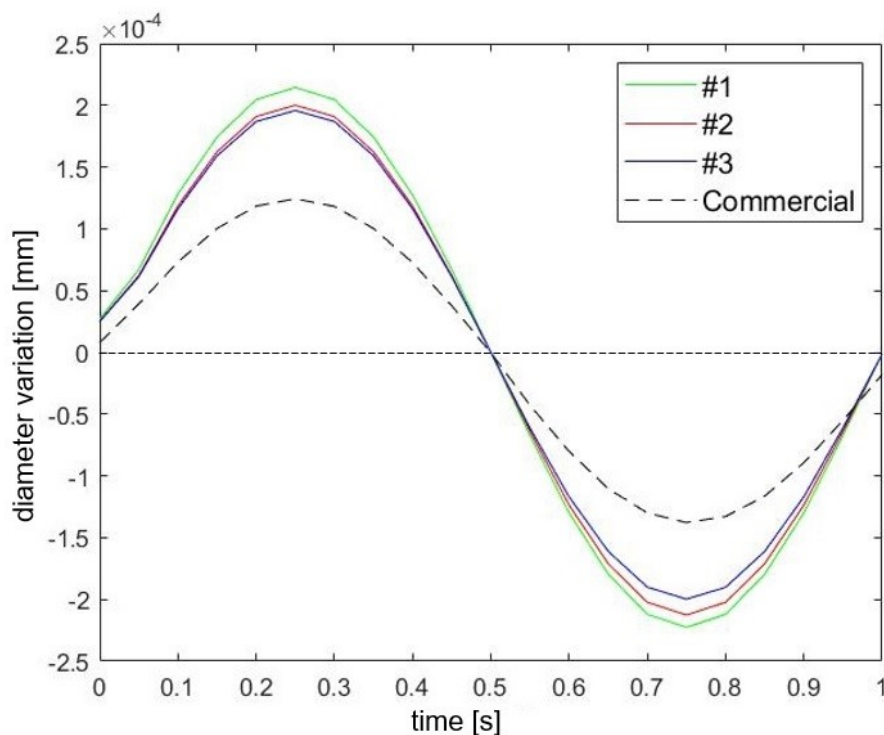


Figure 25. Diameter variation data during the breathing cycle.

3.2 Stent stress states

The maximum principal stress has been reported to investigate the stress exerted in the trachea's tissues during breathing in the presence of the stent. Taking as reference one of the models studied, Figure 26 shows that the trachea's tissues are affected by a very low maximum principal stress. No differences can be seen among the models analysed. However, it is appreciable that cartilage tissue is more rigid than the muscle, which is more deformable. Thus, given that the same pressure is enforced in both tissues, stresses on the cartilage are greater because it provides greater resistance to the same deformation in comparison with the muscular membrane. This difference in stiffness is evident in Figure 26.

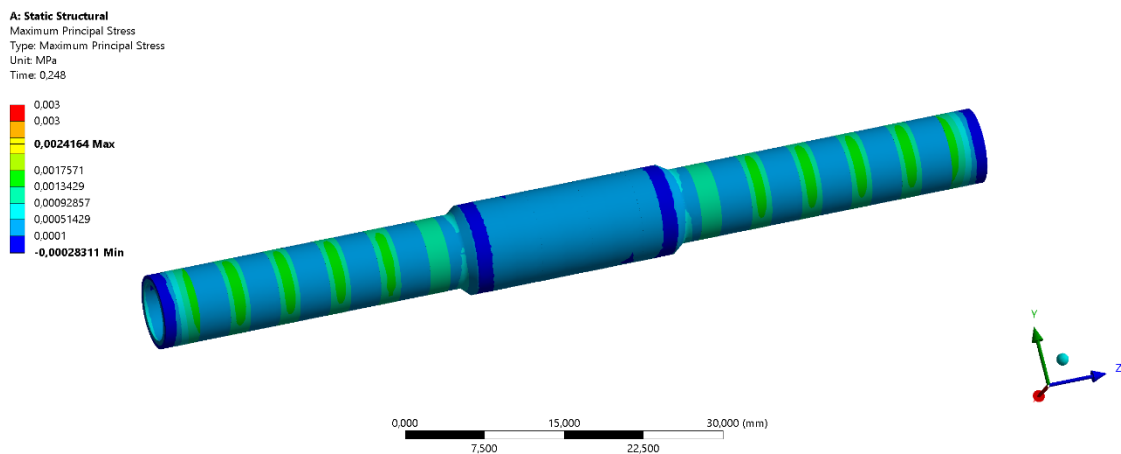


Figure 26. Maximum principal stress during the inhalation phase

Furthermore, all stents were investigated individually to assess the stresses at the level of the ribs, i.e. the parts that are in contact with the inner wall of the trachea. Figure 27 shows that in the ribs, especially with the stent #3 (Figure 27 c)), the maximum principal stress is close to zero. As expected, the commercial Dumon stent (Figure 27 d)) shows a higher value of stress due to the configuration of the device.

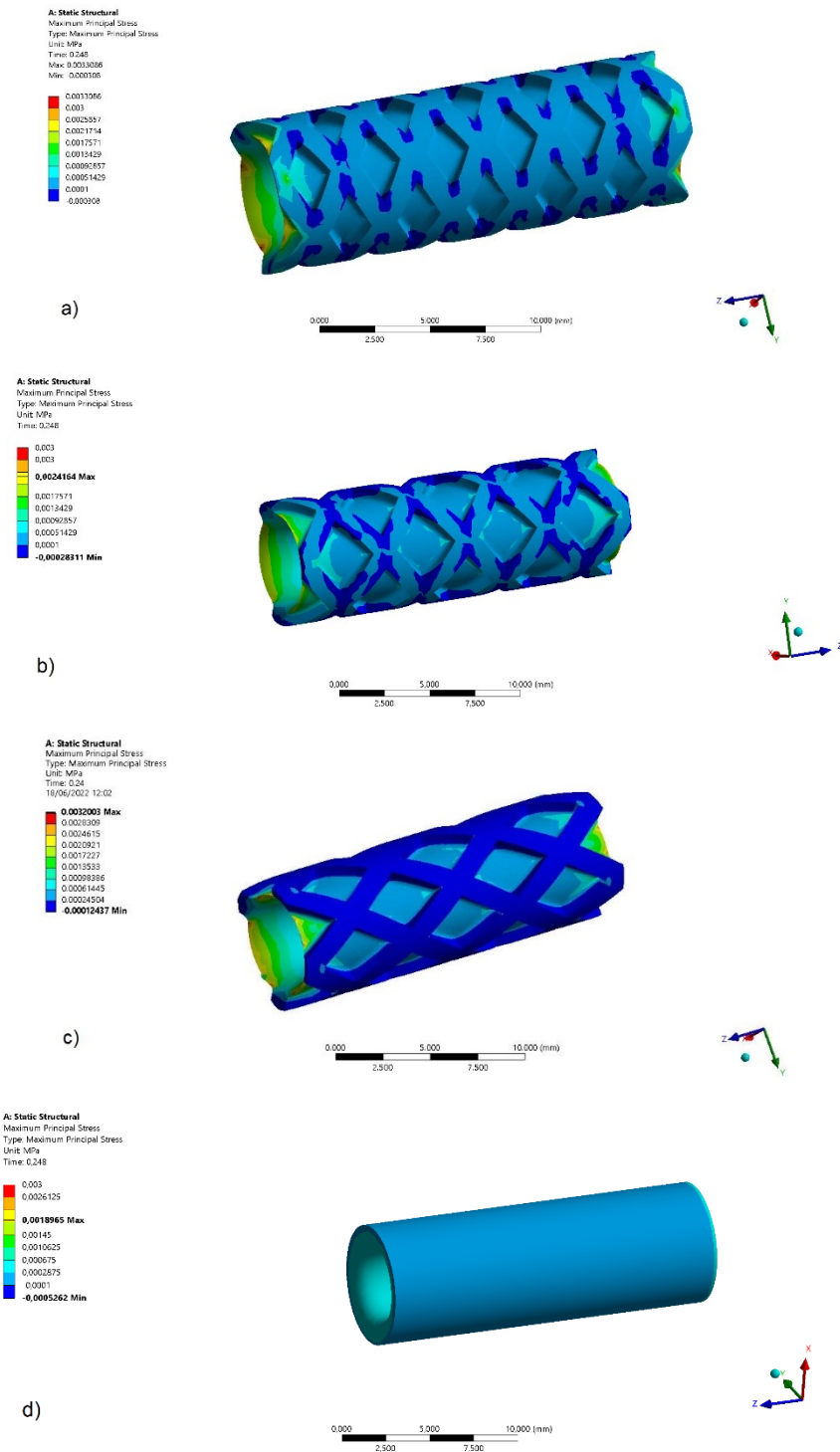


Figure 27. Maximum principal stress (MPa) during the inhalation phase of a) stent #1, b) stent #2, c) stent #3, and d) Dumon's stent.

Figure 27 shows that stress values are close to zero. Therefore, it can be deduced that due to various factors, such as material stiffness, device configuration and thickness, there is no appreciable difference among the different types of new-generation stents. However, a comparison with the commercial Dumon stent

shows that the new generation stents are less stiff, even if this has no remarkable effect on the coupling of the stents with the trachea, being the latter largely less stiff than the stents.

In addition, to confirm that the high stiffness of the devices is far from the stiffness of the trachea an internal pressure and strain plot was performed using a log scale to represent the y-axis (Figure 28-29).

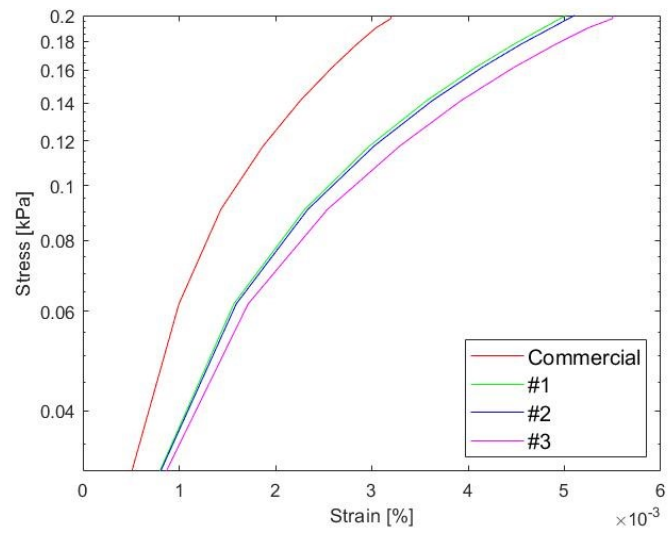


Figure 28. Internal pressure-Strain stent data. Y-axis in log scale.

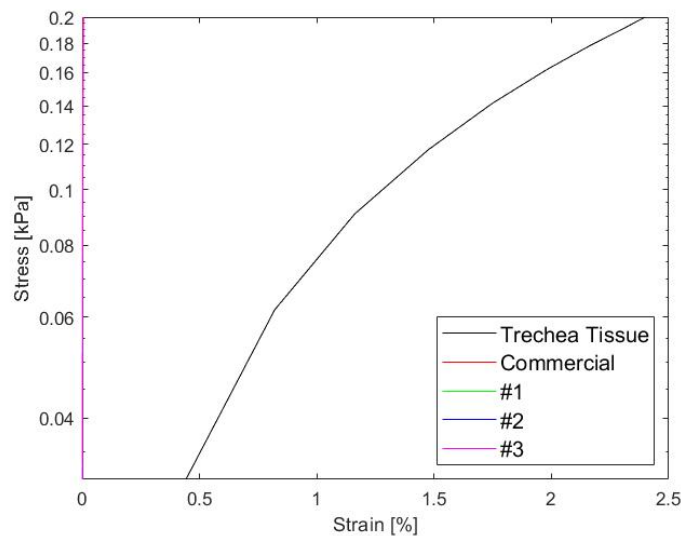


Figure 29. Internal pressure-Strain stent data compared to trachea tissue. Y-axis in log scale.

3.3 Alternative materials

Following the results presented above, it was decided to extend the research towards materials alternative to medical silicone. The materials considered are PDMS and PVA. Two different types of material were taken from both; for PDMS, two compositions were chosen, 5:1 and 10:1, whereas for PVA, in addition to the basic material, an oxidated form using potassium permanganate (KMnO_4) was analysed. Only one model was considered to perform the numerical analyses, the model with stent #2, as no substantial differences occurred between the various stent types evaluated.

The internal pressure vs. strain graph of Figure 30 shows the results obtained from the numerical simulations. It is evident that these materials perform better than medical silicone since the structural stiffness of a stent made of these materials is much lower.

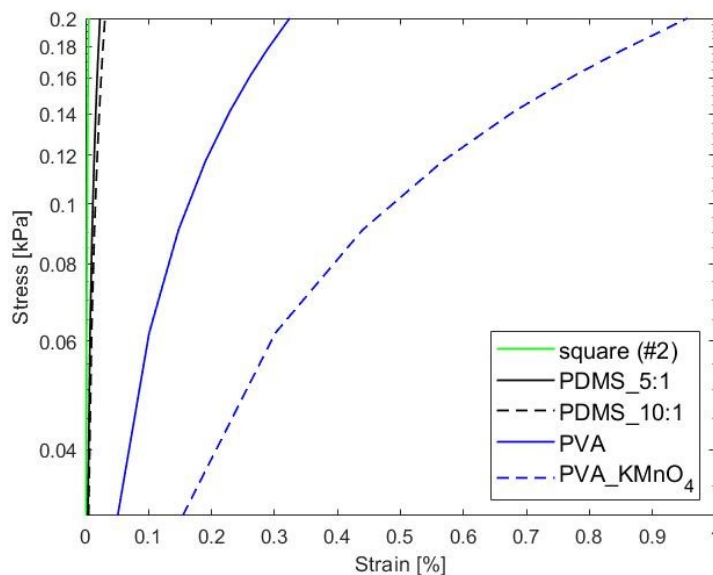


Figure 30. Internal pressure-Strain stent data related of different materials. Y-axis in log scale.

For the two PDMS composition the differences from the medical silicone are present but limited, whereas for the PVA and ox_PVA the differences are appreciable.

A comparison with the trachea tissue was also considered for these materials (Figure 31). The graph shows that the stiffness of ox_PVA stent is more closely to the trachea tissue, thus could be a reasonable option. Moreover, this material results to be a biodegradable hydrogel, thus it can be used as a temporary replacement until the damage will be healed. However, it must be considered that biodegradability is not part of this study and that the suitability of the kinetic of biodegradability should be carefully evaluated before using this type of material.

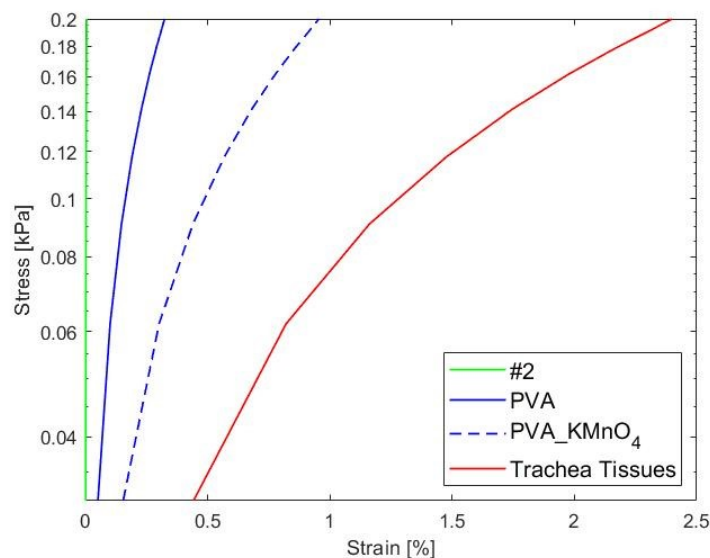


Figure 31. Internal pressure-Strain stent data compared to trachea tissue. Y-axis in log scale.

3.4 Circumferential deformation

Further investigation was performed to provide a numerical perspective of how the circumferential deformation of the device varies between animal and human models. The device made for the animal model was directly scaled from the prototype designed for the human model in the study by Jesús Zurita et al. [30].

However, in the rescaling phase the thickness cannot be changed because 3D printing cannot achieve thicknesses below 0.8mm. Therefore, the analytical estimate of circumferential deformation was conducted assuming two circular sections of equal thickness and different diameter. For the human stent, an inner radius of 9mm was used, while for the rabbit stent the same radius was used in this study, i.e. 2.75mm.

The calculation of the circumferential stress of thin-walled tubes subject to internal pressure is based on the following formula [40]:

$$\sigma = \frac{PD_o}{2t}$$

where P is the internal pressure, D_o is the external diameter and t is the thickness. In this case, the formula gives the maximum circumferential stress on the inner surface. Regarding to the pressure values acting on the inner surface of the trachea, the inspiration peak in the breathing cycle of the different models was taken as a reference. Indeed, in a human breathing cycle, there is a maximum internal pressure in the inhalation phase of approximately 0.5 kPa [41], whereas, as already seen, for the rabbit it is 0.2 kPa. Once the circumferential stress was found for both models, the deformation was derived. The results showed that between animal and human stents the circumferential deformation of the human stent is four times the circumferential deformation of the animal stent.

CHAPTER 4

Discussion and Conclusion

In this work, a FEM-based numerical analysis was used with the objective of evaluating the biomechanical behaviour of a new prototype trachea stent and its interaction with biological tissues. The main intent was to provide results that could be compared with those obtained from experiments on animal models conducted at the University of Zaragoza. The numerical analysis makes it possible to investigate several phenomena without physically reproducing the model of interest in the laboratory, thus saving time and costs. In fact, the aim of developing numerical models is to experiment with alternative methods to the use of animal testing. Therefore, this approach has also remarkable advantages from an ethical point of view. Mathematical models can be used for the preliminary analysis, to reject invalid solutions. However, it must be stressed that numerical simulations start from an idealisation of the real system. Consequently, all the assumptions that are introduced, such as on geometry, load, and materials, may limit the likelihood of the results obtained from the simulations. The approximations and the context in which they are made must always be considered.

Regarding the materials adopted, it is known that different polymers can be used in medicine, exploiting their specific properties [30]. The silicon was used as the primary material tested for the new generation of tracheobronchial stents present in this work. Thereafter, PDMS and PVA were investigated. The use of PDMS

in these devices can offer great advantages, such as biocompatibility, easy manufacturing, and low cost. The nonlinear elastic behaviour is a great advantage that makes PDMS a material of interest in these types of applications [32]. PVA hydrogels were evaluated as a material of interest because of their biodegradability. From the results obtained, it can be deduced that they are good candidates as an alternative to silicone and polydimethylsiloxane (PDMS), offering better mechanical properties as well as the possibility of biodegrading. Based on the results of the numerical analyses developed, the various types of stents presented do not show major differences in terms of mechanical behaviour. Slight differences can be observed between the new stent type and the commercial stent, as the latter was found to be stiffer.

The analytical estimation of radial stiffness between animal and human stents shows that the compliance of the human stent is four times the compliance of the animal stent. Indeed, the human prosthesis is less stiff than the animal one, as it has the same thickness but a larger diameter.

It can be concluded that the computational approach proposed in this work represents a valid tool to test different typologies of stents.

Future improvements will include the assessment of biodegradability for devices made of oxidised PVA. In addition, the possibility of developing a numerical model that can simulate the biological environment of the human trachea may be explored.

Bibliography

- [1] M. W. John A Ormiston, «Of Stents and Scaffolds: Trial Data and the Real World,» *Cardiovascular inventions*, 2016.
- [2] B. M. C. E. D. J. R. G. V. J. Jougon J., «Conservative treatment for postintubation tracheobronchial rupture,» vol. 69, pp. 216-220, 2000.
- [3] A. M. A.L. Rafanan, «Stenting of the tracheobronchial tree,» *Radiol. Clin. N. Am.*, n. 38, p. 395–408, 2000.
- [4] R. G. R. K. J. L. M. W. K. W. R.H. Thornton, «Outcomes of tracheobronchial stent placement for benign disease,» *Radiology*, p. 273–282, 2006.
- [5] E. Y., «Imaging evaluation of laringotracheal stenosis,» *J Otolaringol*, pp. 265-77, 1993.
- [6] D. D. M. D. Grillo HC, «Postintubation tracheal stenosis,» pp. 486-92, 1995.
- [7] G. H.C., «Surgical treatment of postintubation tracheal injuries,» *J Thorac Cardiovasc Surg*, vol. 78, n. 6, pp. 860-875, 1979.
- [8] R. C. D. A. K. R. H. J. R. N. W. J. M. G. Massard G., «Tracheobronchial lacerations after intubation and tracheostomy,» *Ann Thorac Surg*, vol. 61, n. 5, pp. 1483-1487, 1996.
- [9] M. I. B. R. P. A. B. S. J. O. D. I. K. V. Harustiak S., «Tracheal stenosis and its treatment,» *Bratisl Lek Listy*, vol. 100, n. 6, pp. 291-295, 1999.
- [10] M. S. L. F. G. B. L. Fuccio, «Development of a prediction model of adverse events after stent placement for esophageal cancer,» *Gastrointest. Endosc.*, vol. 83, n. 4, p. 746–752, 2016.
- [11] Q. J. B. L. v. G. H. G. J. E. M. H. C. Jacobs J.P., «The role of airway stents in the management of paediatric tracheal, carinal and bronchial disease,» *Eur J Cardiothoracic Surg*, vol. 18, pp. 505-512, 2000.
- [12] K. Y. T. S. T. I. N. M. K. Y. Y. Tanaka, «Recent advancements in esophageal cancer treatment in Japan,» *Ann. Gastroenterol. Surg.*, vol. 2, n. 4, p. 253–265, 2018.
- [13] D. M. D.J. Minnich, «Anatomy of the trachea, carina, and bronchi,» *Thorac. Surg. Clin.*, vol. 17, n. 4, p. 571–585, 2007.
- [14] T. A. J.L. Soon, «Total tracheal resection for long-segment benign tracheal stenosis,» *Ann. Thorac. Surg.*, vol. 85, n. 2, p. 654–656, 2008.
- [15] J. G. M. M. M. P. I. Delgado, «Clinic, diagnosis and treatment of tracheal stenosis,» *An. Pediatr. (Barc.)*, vol. 70, n. 5, p. 443–448, 2009.

- [16] L. L. J. S. E. C. S. P. Marques, «Tracheal resection with primary anastomosis: 10 years experience,» *Am. J. Otolaryngol*, vol. 30, n. 6, p. 415–418, 2009.
- [17] I. D.-x. Z. ., C.-g. W. Y.-b. C. ., D. S.-y. M. J. F. T. a. J.-a. H. Jun-hong Jiang, «"A Pilot Study of a Novel through-the-Scope Self-Expandable Metallic Airway Stents Delivery System in Malignant Central Airway Obstruction,"» *Canadian Respiratory Journal*, vol. 2019, pp. 1-7, 2019.
- [18] J. U. J. E. V. C. L. L. M. M. F. Sun, «Endotracheal stenting therapy in dogs with tracheal collapse,» *Vet. J.*, vol. 175, pp. 186-193, 2008.
- [19] H. H. U. L. C. W. M. T. R. H. K. P. J. Rieger, «Treatment of benign and malignant tracheobronchial obstruction with metal wire stents: experience with a balloon-expandable and a self-expandable stent type,» *Cardiovasc. Intervent. Radiol.*, vol. 27, pp. 339-343, 2004.
- [20] J. L. E. M. S.A. Zakaluzny, «Complications of tracheobronchial airway stents,» *Otolaryngol. Head Neck Surg.*, vol. 128, n. 4, pp. 478-448, 2003.
- [21] J. P. V. M. F. J. L. K. U. Sigwart, «Intravascular stents to prevent occlusion and restenosis after transluminal angioplasty,» *N. Engl. J. Med.*, vol. 316, pp. 701-706, 1987.
- [22] C. Y. S. L. Q. Y. G. W. Tingzhang Hu, «Biodegradable stents for coronary artery disease treatment: Recent advances and future perspectives,» *Materials Science & Engineering C*, vol. 91, pp. 163-178, 2018.
- [23] G. F. Y. Z. G. W. T. C. Qian Wang, «Computational and experimental investigation into mechanical performances of Poly-L-Lactide Acid (PLLA) coronary stents,» *journal of the mechanical behavior of biomedical materials*, pp. 415-427, 2017.
- [24] B. W. R. G. Bucher RM, «Experimental reconstruction of tracheal and bronchial defects with stainless steel wire mesh,» *J Thorax Surg*, vol. 21, n. 6, pp. 572-583, 1951.
- [25] S. D. R. A. C. C. Indolfi, «Bioresorbable vascular scaffolds – basic concepts and clinical outcome,» *Nat. Rev. Cardiol.*, vol. 13, pp. 719-729, 2016.
- [26] C. B. M. A. Y. Z. R. S. H. T. Y. S. Y. O. M. Y. P. S. E. Tenekecioglu, «From drug eluting stents to bioresorbable scaffolds; to new horizons in PCI,» *Expert Rev. Med. Devices*, vol. 13, n. 3, pp. 271-286, 2016.
- [27] L. MG., «Pulmonary physiology,» *McGraw-Hill Education*, 2018.
- [28] C. A. Johnson-Delaney, «Rabbit Respiratory System: Clinical Anatomy, Physiology and Disease».
- [29] L. Novotny, M. Crha, P. Rauser, A. Hep, J. Misik, A. Necas e D. Vondryš, «Novel biodegradable polydioxanone stents in a rabbit.,» *Thorac. Cardiovasc. Surg.*, 2012.

- [30] C. S.-M. C. D.-J. J. L. L.-V. Jesús Zurita-Gabasa, «A Parametric Tool for Studying a New Tracheobronchial Silicone Stent Prototype: Toward a Customized 3D Printable Prosthesis,» 2021.
- [31] C. Cardoso, C. Fernandes, R. Lima e J. Ribeiro, «Biomechanical analysis of PDMS channels using different hyperelastic numerical constitutive models.,» *Mech. Res. Commun.*, 2018.
- [32] A. S. P. S. J. R. E. S. C. R. L. Inês Miranda, «Properties and Applications of PDMS for Biomedical Engineering: A Review,» *Functional Biomaterials*, 2021.
- [33] S. Bianchi Vearick, K. Bendo Dem' trio, R. Gastal Xavier, A. Moreschi, A. Frotta Muller, P. Stefani Sanches e L. Loureiro dos Santos, «Fiber-reinforced silicone for tracheobronchial stents: An experimental study.,» *Mech. Behav. Biomed. Mater.*, 2018.
- [34] C. R. F.-P. E. F. M. D. G. M. a. M. J. Chaure, «On Studying the Interaction Between Different Stent Models and Rabbit Tracheal Tissue: Numerical, Endoscopic and Histological Comparison,» *Annals of Biomedical Engineering*, 2016.
- [35] C. S. E. P. R. F.-P. F. L. M. D. G. M. M. Malvè, «Modelling the air mass transfer in a healthy and a stented rabbit trachea: CT-images, computer simulations and experimental study.,» *International Communications in Heat and Mass Transfer*, 2014.
- [36] Z. Wang, «Polydimethylsiloxane Mechanical Properties Measured by Macroscopic Compression and Nanoindentation Techniques,» 2011.
- [37] C. Horejs, «Biomaterials: don't stress over it.,» *Nat. Rev. Mater.*, 2017.
- [38] S. B. E. S. M. F. V. M. R. D. C. A. P. P. G. P. Silvia Todros, «Time-dependent mechanical behavior of partially oxidized polyvinyl alcohol hydrogels for tissue engineering,» 2021.
- [39] F. Dumon, «A dedicated tracheobronchial stent.,» *Applied Sciences*, 1990.
- [40] J. Goodman, «Mechanics applied to Engineering,» 1914.
- [41] R. D. P. P.-V. A. G. M. D. M. MALVE', «FSI Analysis of the Coughing Mechanism in a Human Trachea,» *Annals of Biomedical Engineering*, 2010.

